

An study on emission and origin source of Volatile Organic Compounds (VOCs)

A thesis submitted in partial fulfilment of
the requirements for the degree of

Doctor of Philosophy

by

Nidhi Tripathi

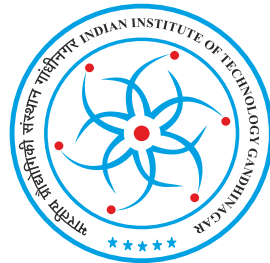
(Roll No. xxxxxxxx)

Under the guidance of

Dr. Lokesh Sahoo

Space and Atmospheric Division

Physical Research Laboratory, Ahmedabad, India.



DISCIPLINE OF PHYSICS

INDIAN INSTITUTE OF TECHNOLOGY GANDHINAGAR, GUJARAT, INDIA

2020

Dedicated to my parents



Declaration

I declare here that this thesis report represents my own ideas in my own words and I have included others ideas with appropriate citations from original sources. I also declare that I have followed all principles of academic honesty and integrity and have not misrepresented or fabricated or falsified any idea/fact/source/data in my submission. I understand that any violation of the above can cause disciplinary action by the Institute and can also evoke penal action from the sources which have thus not been properly cited or from whom proper permission has not been taken when needed.

Nidhi Tripathi

(Roll No: xxxxxxx)

Date: March 3, 2024

CERTIFICATE

It is certified that the work contained in the thesis titled "**An study on emission and origin source of Volatile Organic Compounds (VOCs)**" by **Ms. Nidhi Tripathi** (Roll No. 11330014), has been carried out under my supervision and that this work has not been submitted elsewhere for a degree.

Dr. Lokesh Sahoo
(Thesis Supervisor)

Professor,
Space and Atmoshpere Division
Physical Research Laboratory,
Ahmedabad, India.

Date:

Acknowledgements

This thesis is the culmination of my journey of Ph.D which was just like climbing a high peak step by step accompanied with encouragement, hardship, trust, and frustration. When I found myself at top experiencing the feeling of fulfillment, I realized though only my name appears on the cover of this dissertation, a great many people including my family members, well-wishers, my friends, colleagues and various institutions have contributed to accomplish this huge task.

At this moment of accomplishment I am greatly indebted to my research guide, Dr. Prof. Lokesh Sahu, who accepted me as his PhD student and offered me his mentorship, motherly love and care. This work would not have been possible without his guidance and involvement, his support and encouragement on daily basis from the start of the project till date. Under his guidance I successfully overcame many difficulties and learnt a lot. His own zeal for perfection, passion, unflinching courage and conviction has always inspired me to do more. He has taught me another aspect of life, that, “goodness can never be defied and good human beings can never be denied”. For all these, I sincerely thank him from bottom of my heart and will be truly indebted to him throughout my life time. My earnest thanks to Dr. Arvind Singh, reader at PRL and Prof. S. N. Tripathi, Prof. at IIT-Kanpur, for supporting and sponsoring throughout the Ph.D. work. I am grateful for their valuable advice, constructive criticism, positive appreciation and counsel throughout the course of the investigations which led to the successful completion of the research work. No research is possible without infrastructure and requisite materials and resource provided at PRL. For this I extend thanks to PRL for providing me with the requisite institutional facilities throughout my research tenure. I greatly appreciate and acknowledge the support received from few institutions and laboratories. Most of the results described in this thesis would not have been obtained without their support. I am equally thankful to Prof. S.N. Tripathi from IIT-kanpur, Prof. **name** of IIT-Delhi, space and atmospheric division and Prof. **name** Manvrachana University for providing basic infrastructure and the place for the sample collection. My sincere thanks to Prof. Prof. **name of prof from france or U.K.** for his valuable guidance, timely

suggestions and support during the delhi campaign.

I am grateful to Prof. Ramachandan, Prof. Pallamraju **name of other professors of ur division** for their support, understanding, encouragement and love when it was most required. All the other Non-teaching staff have helped me and thanks are due to all of them for their silent contributions in particular Mrs. **name of staff members from ur division and PRL whom u want to give credit** for their sincere encouragement and support throughout my thesis writing. It's my fortune to gratefully acknowledge the support of my friends, **name of ur friends** for their support and generous care throughout the research tenure. They were always beside me during the happy and hard moments to push me and motivate me. Special thanks are extended to Shefali and Ayan. Big thanks to all my fellow colleagues and friends, particularly, **name** for their co-operation and support. Finally, I acknowledge the people who mean a lot to me, my parents, **name** and sister, brother and jiju, for showing faith in me and giving me liberty to choose what I desired. I salute you all for the selfless love, care, pain and sacrifice you did to shape my life. Although you hardly understood what I researched on, you were willing to support any decision I made. I would never be able to pay back the love and affection showered upon by my parents. Also I express my thanks to my brother Golu, and sister Goli for their support and valuable prayers. I am also thankful to Ravi for the support till now. I consider myself the luckiest in the world to have such a lovely and caring family, standing beside me with their love and unconditional support. I thank the Almighty for giving me the strength and patience to work through all these years so that today I can stand proudly with my head held high.

Nidhi Tripathi

Abstract

Write abstract of your thesis.

Keywords: Volatile Organic Compound (VOCs), Biogenic VOCs, PTR-TOF-MS

Contents

Acknowledgements	i
Abstract	iii
Contents	v
List of Figures	vii
List of Tables	x
1 Introduction	3
1.1 Introduction to the atmospheric physics	3
1.2 Works done in the field	3
1.3 What motivates you to work in the field	3
2 Instrumentation	5
2.1 Introduction	5
2.2 Objective	7
2.3 Methodology	8
2.3.1 PTR-TOF-MS	9
2.4 Works done and future plans	13
3 Elevated levels of biogenic non-methane hydrocarbons in the marine boundary layer	17
3.1 Introduction	17
3.2 Campaign and Experimental Methodology	20
3.3 Results and Discussion	24

3.3.1	Time series and diurnal variations of NMHCs	24
3.3.2	Latitudinal variation of NMHCs	30
3.3.3	Role of ocean productivity	32
3.3.4	Dependence of NMHCs on meteorological parameters . . .	33
3.4	Comparison with other oceanic regions	34
3.5	Conclusion	35
4	Work3	45
5	Work4	47
6	Summary and Future Directions	49
6.1	Summary	49
7	Appendix	51
7.1	Title of second appendix	51
Bibliography		53
List of publications		61

List of Figures

2.1	Schematic diagram exhibiting temperature and light dependence of BVOCs emissions (Source: Hewitt et al. 2009)	7
2.2	A block diagram showing important components of the PTR-TOF-MS.	9
2.3	Schematic diagram of drift tube of PTR-TOF-MS instrument.	10
2.4	Path of the ions from Einzel-lens to TOF.	11
2.5	Multi Channel Plate	12
2.6	Ongoing and proposed sampling sites/regions in India	14
2.7	Branch enclosure set up diagram	15
3.1	Emission from phytoplankton and dissolved organic carbon (DOC) present in ocean water is an important natural source of many non-methane hydrocarbons (NMHCs) in the marine boundary layer (MBL). Phytoplankton takes nutrients from the seawater and zooplankton grazes phytoplankton, and DOC is produced by phytoplankton during photosynthesis. Photo-oxidation of DOC leads to production of NMHCs in seawater. Diatom and cyanobacteria directly produce light NMHCs in the seawater. The exchange of gases from seawater to air is controlled by prevailing meteorological conditions but mainly wind by the wind speed. VOCs released in the marine atmosphere are oxidized by reaction with OH radical and can produce ozone and secondary organic aerosol (SOA) which affect the radiation budget of the earth's atmosphere.	19

3.2	Cruise track, different sections (A, B, C and D), air sampling (red circle) and water sampling (green square) locations over the Arabian Sea during 15 April-2 May 2017	22
3.3	7-day back trajectories at 100 m above mean sea level (amsl) over different air sampling locations.	24
3.4	Time series of the mixing ratios (ppbv) of (a) ethene, propene and total (sum of 100 different diatom species measured at 1-13 stations), (b) 1-butene, 1-pentene and Cis-2-butane (c) ethane and propane, (d) solar radiation flux and relative humidity, (e) ambient temperature and wind speed and (f) latitude and longitude of air sampling locations along the cruise track	25
3.5	Average diurnal patterns of NMHCs mixing ratio, solar flux and ambient temperature over the Arabian Sea during 15 April-2 May 2017. The diurnal dependencies of NMHCs and meteorological parameters measured over the Bay of Bengal during monsoon/post-monsoon (BOB 2002) and winter (BOB 2003) seasons are also plotted for the comparison. Bay of Bengal data are taken from Sahu et al., (2010).	26
3.6	Scatter plots of (a) ethene versus propene, (b) ethene versus ethane and (c) ethane versus propane measured during the present study, BOB 2002 and BOB 2003 campaigns	27
3.7	The relations of ethene and propene with (a, b) solar flux, (c, d) wind speed, (e, f) temperature and (g, h) equivalent potential temperature (EPT). The Box-whiskers represent statistics of ethene and propene for higher and lower values of solar flux, ambient temperature, wind speed and EPT	28
3.8	Comparison with the mixing ratios of ethene and propene measured in the marine boundary layer (MBL) of different oceanic regions of world. Further details of the data and references are given in Table S1.	29

3.9 Calibration plot of NMHCs. All the above set values of NMHCs are showing good relationships with area under curve.	40
3.10 Chromatograms of the VOCs analyzed by TD-GC-FID for air samples collected during the day and night. The amplitude and area under the peaks of alkene during daytime were greater than those for nighttime.	41
3.11 Average wind stream line at 1000 hpa pressure level and sea surface temperature (SST) during April using NCEP data over the Arabian sea for different cruise track A, B, C and D. For cruise track A, the flow of wind is from the north (higher productive region) which also contribute to high mixing ratios of alkenes.	41
3.12 The box whisker plots show that the mean value of ethene and propene with solar flux, temperature and wind speed over the Bay of Bengal during post-monsoon (September-October) BOB 2002 campaign. Here solar flux, ambient temperature and wind speed have been taken less than and greater than 300 w m^{-2} , 28°C and 6 m s^{-1} , respectively.	42

List of Tables

3.1	The average \pm standard deviation of the mixing ratios of NMHCs (ppbv) and meteorological parameters measured along four different tracks over the Arabian Sea during 15 April-2 May 2017.	37
3.2	The average \pm standard deviation of the mixing ratios of NMHCs (ppbv) measured over open ocean and coastal regions, and for daytime and nighttime over the Arabian Sea.	38
3.3	List of water sampling stations where abundance of diatom and cyanobacteria community (cells L-1) was measured which are known to contribute the production of ethene and propene in the seawater (Ratte et al., 1993)	39
3.4	The average \pm standard deviation of the mixing ratios of NMHCs (ppbv) measured over open ocean and coastal regions, and for daytime and nighttime over the Arabian Sea.	43

List of terms used in the thesis

Short name/ Symbol	Definition / meaning
VOC	Volatile Organic Compound
BVOC	Biogenic Volatile Organics Compound
PTR-TOF-MOS	Proton Transfer of Mass Spectroscopy
MHD	Magnetohydrodynamics
CMB	Cosmic Microwave Background
BBM	Biermann Battery Mechanism
BBN	Big Bang Baryogenesis
CME	Chiral Magnetic Effect
ChMHD	Chiral Magnetohydrodynamics
CVE	Chiral Vortical Effect
CVW	Chiral Vortical Waves
CAW	Chiral Álfven Waves
CMW	Chiral Magnetic Waves
CSE	Chiral separation effect
EM	Electromagnetic
SM	Standard Model
EW	Electroweak
GUT	Grand Unified Theory
QCD	Quantum Chromodynamics
BAU	Baryon Asymmetry of the Universe

Short name/ Symbol	Definition / meaning
n D	n dimensional space
kpc/Mpc	kiloparsec/megaparsec
eV	electron volt
keV	kilo electron volt
MeV	mega electron volt
GeV	giga electron bolt
H	Hubble constant
ρ	Matter energy density
ρ_γ	Radiation energy density
ω	vorticity vector
m_p	mass of the ions
k_B	Boltzmann's coefficient
c	speed of light
σ	electrical conductivity
α	fine structure constant
m_e	electron mass
μ	micro
\hbar	reduced Planck constant ($\hbar = h/2\pi$)
M_{pl}	Planck Mass
G	Gauss
\Re	set of Real number

Chapter 1

Introduction

1.1 Introduction to the atmospheric physics

write here Introduction

1.2 Works done in the field

1.3 What motivates you to work in the field

Chapter 2

Instrumentation

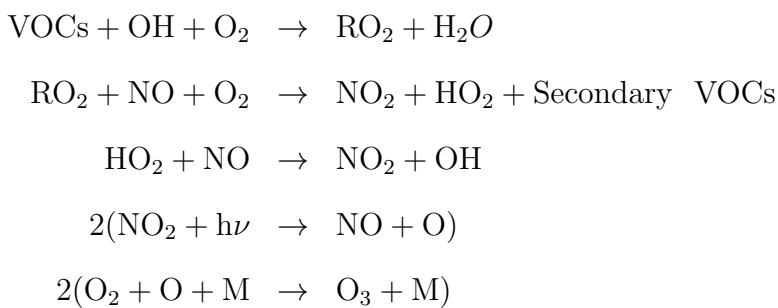
2.1 Introduction

The atmosphere is a thin envelope of air surrounding the earth's surface. Primarily, it is composed of nitrogen N₂ (78%), oxygen O₂ (21%) and argon Ar (0.93%) gases known as the major constituents. The remaining constituents (< 1%) are subdivided into minor gases (e.g., CO₂, He, Ne, etc., in order of ppmv) and trace gases (e.g., O₃, CO, N₂O, volatile organic compounds (VOCs), etc. in the range of pptv-ppbv). Despite their low atmospheric abundances, most of the tracegases have significant direct and indirect effects on climate and air quality. Among the trace gases, VOCs play important role in the earth's atmosphere. VOCs represent numerous organic compounds which have very low boiling point or high vapor pressure at room temperature. However, with large spatio-temporal variations, mixing ratios of VOCs vary in the range of pptv-ppbv in the earth atmosphere. VOCs are classified in different categories such that non-methane hydrocarbons (NMHCs, for example: Alkanes C_nH_{2n+2}, Alkenes C_nH_{2n}, Alkynes C_nH_{2n-2}, Aromatics Ring, etc.), oxygenated-VOCs (OVOCs) (for example: Aldehydes, Ketones, Alcohols, etc.) and hydrocarbons containing N, S and halogens (e.g. CH₃CN, DMS, methyl chloride).

There are many sources of both natural and anthropogenic origins which emit VOCs. The major natural (or biogenic) sources include emissions from the terrestrial vegetation, ocean, volcanic eruption, decomposition of plant materials,

etc. The terrestrial vegetations are plant, shrub, grass and crop. For example, coniferous forest emits large fraction of OVOCs like methanol, acetone, ethanol and acetaldehyde (Barker et al. 1999, Golden et al. 1993). Most of trees emit high amount of VOCs known as biogenic-VOCs (BVOCs) such as isoprene and terpenes. Shrub and grassland mainly emit terpenoids. Drying or cutting grasses release OVOCs along with isoprene, monoterpenes ($C_{10}H_{16}$) and sesquiterpenes ($C_{15}H_{24}$). Emission from dissolved organic carbon (DOC) is a primary source of oceanic OVOCs (Singh et al., 2000). DOC is formed due to the decomposition of plant and animal organisms also known as phytoplankton and zooplankton. Di methyl Sulphide (DMS), methyl iodide, isoprene, alkanes and alkene are main VOCs released from the ocean waters. The major anthropogenic sources are fossil fuel combustion, biomass burning and industrial processes. Biogenic sources account for 85-90 % in the global budget of VOCs. The most widely accepted global budget estimates for biogenic and anthropogenic sources are about 1150 Tg C/yr⁻¹ and 150 Tg C/yr⁻¹, respectively (Guenther et al., 2012).

In the atmosphere, VOCs are oxidized by hydroxyl radical (OH) leading to formation of ozone in the presence of sunlight and NO_x ($= NO + NO_2$). However, mostly higher molecular weight VOCs, are important precursors of secondary organic aerosols (SOA). A typical set of reactions leading O_3 and SOA formation from VOCs is given below.



As mentioned that the BVOCs make a dominant fraction of global VOCs. However, not only the atmospheric variability but also the emissions depend on environmental and meteorological parameters. Among several meteorological pa-

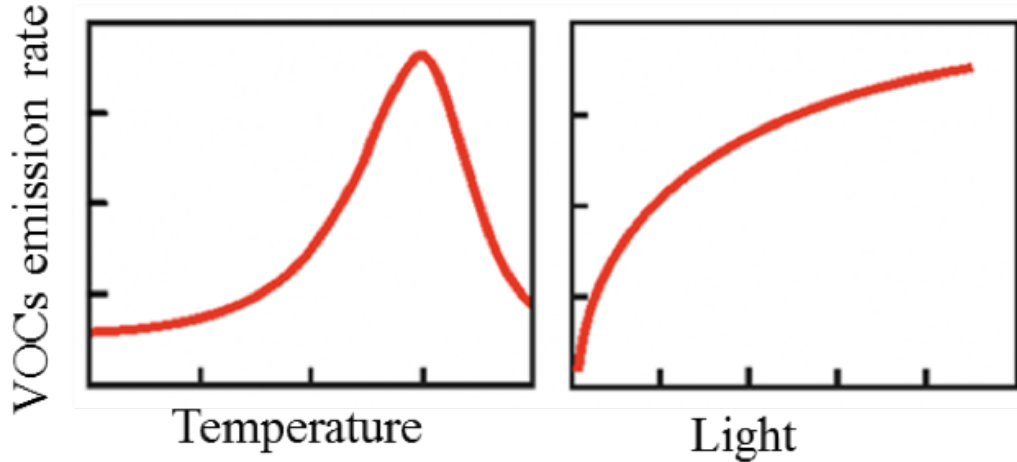


Figure 2.1: Schematic diagram exhibiting temperature and light dependence of BVOCs emissions (Source: Hewitt et al. 2009)

parameters, temperature and sunlight play major roles in determining the emission of BVOCs (as shown in Figure 2.1). For example, emission of isoprene from the plants strongly depends on both temperature and sunlight. In addition to general dependence on temperature and sunlight, the emissions show complex relations with change in other meteorological parameters and weather conditions. It has been reported that a burst (lasting few seconds) of acetaldehyde and some other OVOCs occurs during light to dark transition period. However, exact mechanisms of such emissions are not determined which lead to large uncertainties in emission estimates (Holzinger et al. 2000). Basically, plants synthesize and store BVOCs in the presence of sunlight and when temperature increases they start releasing BVOCs after particular temperature (or a threshold). As temperature increases the emission rate also increases until it reaches saturation. It has been reported that the optimum temperature for highest isoprene emission occurs varies between 35 and 40 oC (Guenther et al. 1993; Harley et al. 1996).

2.2 Objective

According to the emissions models, the contribution of BVOCs from tropical region is estimated to be 80% (large uncertainties). The large uncertainties in

global estimates of BVOCs are mainly due to lack of observations and hence validation of sensitivity of BVOCs emission to meteorological parameters in most parts of the globe. The dependence of BVOCs on meteorological parameters such as temperature, light, humidity, etc. has been rarely reported over South Asia region. In particular, lack of representative parameterization of BVOCs emission from tropical biosphere is one of the largest sources of uncertainty in chemistry-climate model (IPCC, 2013). Thus far, study of VOCs in India is very limited targeting only anthropogenic emission. Study of atmospheric variability of VOCs in context of emissions from biogenic sources has not been reported over Indian subcontinent. Objective of my research is mainly focused on atmospheric variability of VOCs (mainly BVOCs) and emission characteristics of BVOCs in different environments of India.

2.3 Methodology

There are several techniques used for the measurement of VOCs present in the atmosphere. VOCs consist of numerous compounds and there is no single technique or method which can be used to detect all VOCs. Most of the measurements of VOCs have been done using gas chromatography (GC) coupled with a flame ionization detector (FID). Recently, the proton transfer reaction-mass spectrometry (PTR-MS) technique has been used for the sensitive and rapid online measurements of VOCs both in the field and laboratory experiments. In PRL, we use the Proton Transfer Reaction Time of Flight Mass Spectrometer (PTR-TOF-MS) and Thermal Desorption-Gas Chromatography-Flame Ionization Detector (TD-GC-FID) instruments for online and offline measurements of VOCs. So far, I have focused to learn the principle and operational details of PTR-TOF-MS. My understanding about the TD-GC-FID technique is very preliminary and I am learning more details. Here, I have described important parts of PTR-TOF-MS instrument only.

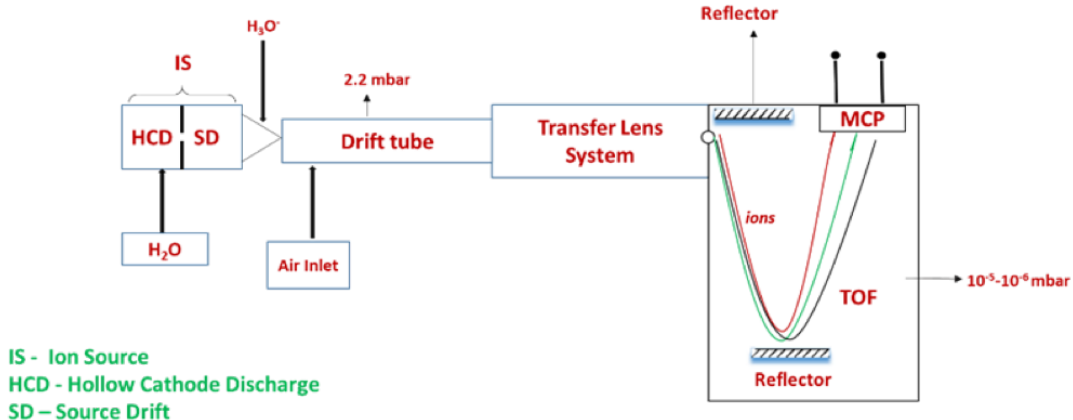


Figure 2.2: A block diagram showing important components of the PTR-TOF-MS.

2.3.1 PTR-TOF-MS

As its name proton transfer reaction (PTR), gaseous molecules present in air are ionized by the transfer of proton. Subsequently, TOF provides separation of different VOCs according to their masses.

The transfer of proton from protonated water (H_3O^+) to VOC is a soft ionization method hence fragmentation is negligible. A block diagram of PTR-TOF-MS instrument is presented in (Figure 2.2). The main parts of the PTR-TOF-MS are:

1. Ion Source
2. Drift tube
3. Analyzing system

Details of these parts are as follows:

1. **Ion Source:** Ion Source is the device where atomic and molecular ions required for a reagent ion (H_3O^+) are produced. Ion source are divided into two chambers namely hollow cathode discharge (HCD) and source drift (SD). Water vapor (H_2O) enters into HCD and gets ionized (H_2O^+). The flow of water vapor is maintained at 5-10 cm^3/min . The pressure inside the HCD is maintained at 1 mbar. Main reactions in HCD and SD are

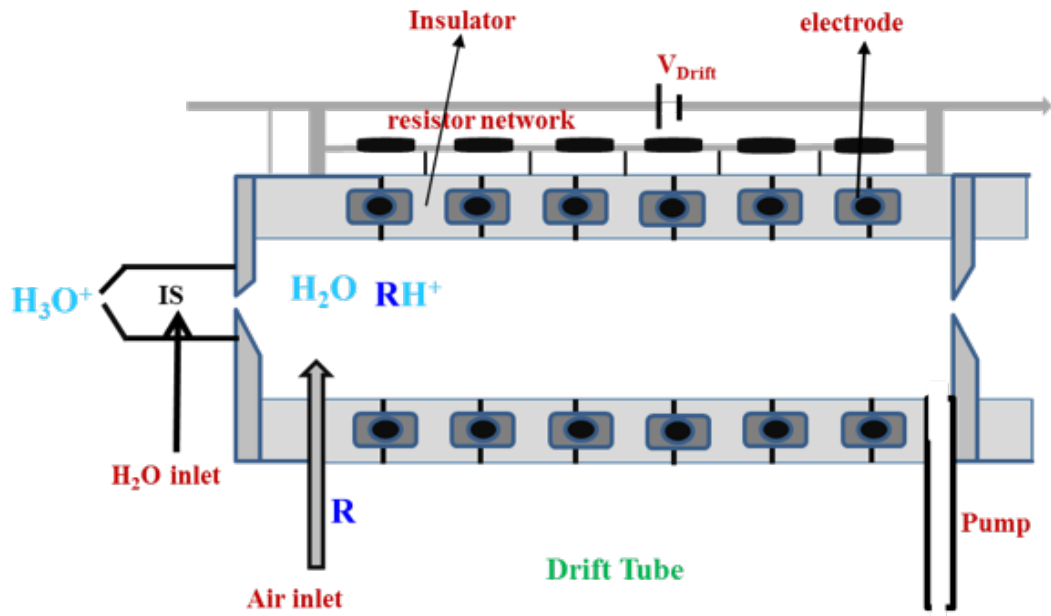
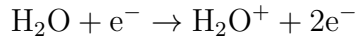
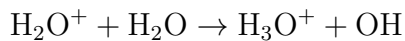


Figure 2.3: Schematic diagram of drift tube of PTR-TOF-MS instrument.

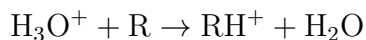
described as here.



In HCD the water molecule can fragment in H_2O^+ , H_2^+ , OH^+ and O^+ . H_2^+ is a minor product. In SD region, H_2O is converted into H_3O^+ by fast reaction at temperature 300K.



2. Drift tube: Drift Tube is a critical part of the PTR-TOF-MS instrument where a VOC are ionized to VOC-H^+ (see Figure 2.3). Typically, the diameter of the drift tube is 4 cm and the length is 9 cm. The temperature of the drift tube is maintained approx. 60°C. The inlet for the air sample is connected to the drift tube. The flow rate of the sample is set at about 25-35 ml/min. The protonated water (H_3O^+) transfers the proton to different species according to their proton affinity (PA). The proton transfer reaction can be described by following reaction.



Where “R” represents a gas compound but mostly VOCs. The PA of H_2O is

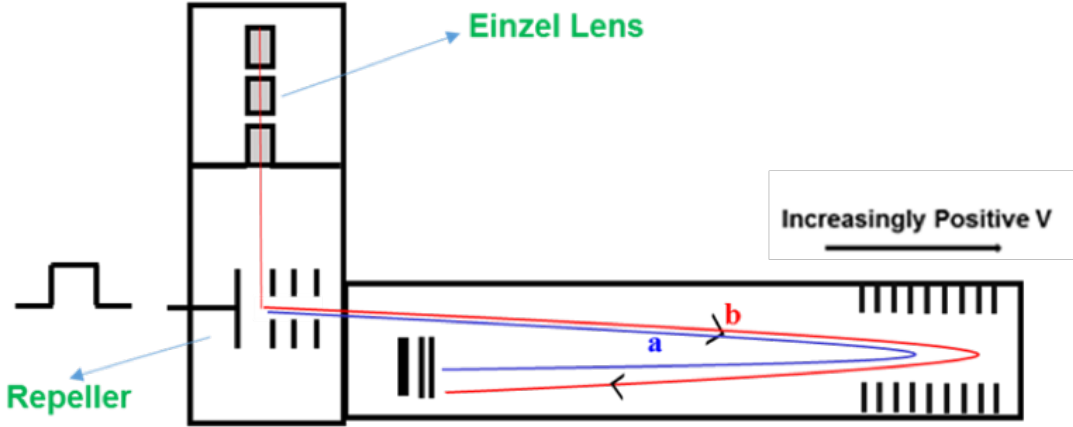


Figure 2.4: Path of the ions from Einzel-lens to TOF.

691kJ/mole (166kcal/mole). So this reaction (or transfer of proton) occurs when the PA of R is greater than that of water.

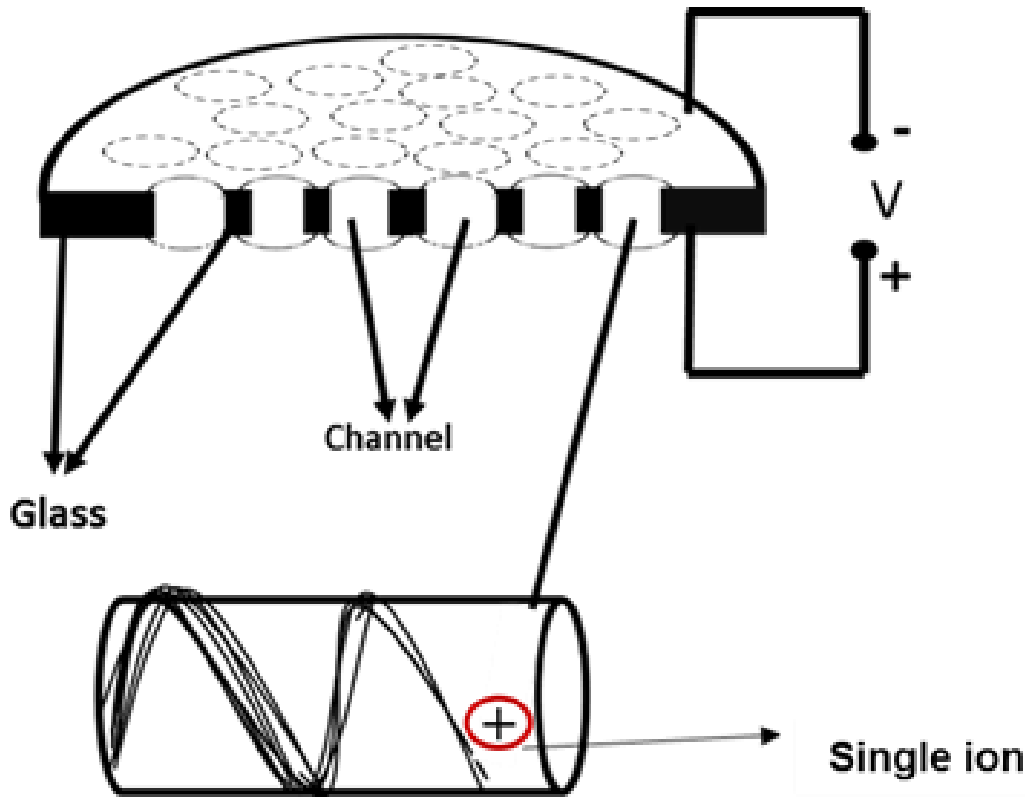
3. Analyzing system: The analyze system consists of (1) Ion Transfer lens, (2) TOF and (3) Multi-Channel Plate (MCP) detector. The functions of each of these components are briefly described as here. The TOF analyzer uses an electric field to accelerate the ionized VOCs through the same potential and then measures the time taken to reach the detector. In TOF, the heavier ions move with lower speeds than those of lighter species. When an ion enters the TOF region its potential energy is converted into the kinetic energy.

$$eV = \frac{1}{2}mv^2$$

Where V = voltage of repeller, v = velocity of ions, m = mass of the ions

Suppose the length of the flight tube is l and the time taken by the ions to reach the detector is t then velocity is

$$\begin{aligned} v &= \frac{l}{t} \\ \Rightarrow eV &= \frac{1}{2}m \left(\frac{l}{t} \right)^2 \\ \Rightarrow t &= \frac{l}{\sqrt{2V}} \sqrt{\frac{m}{z}} \\ \Rightarrow t &= k \sqrt{\frac{m}{z}}, \end{aligned}$$



Mult Channel Plate

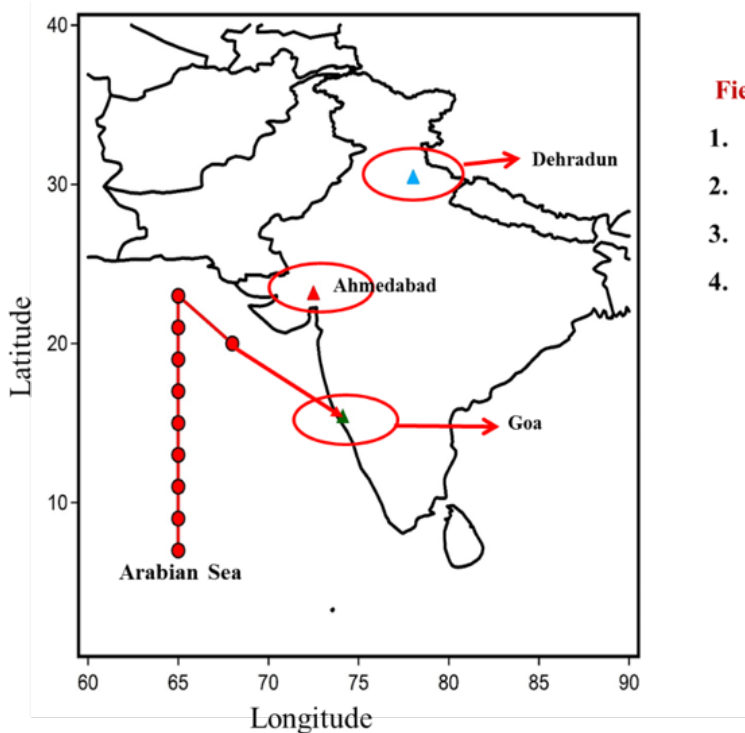
Figure 2.5: Multi Channel Plate

where $k = l/\sqrt{2V}$ A series of electrodes known as reflectron or array of reflectron is used at the end (bottom) of the TOF. The potential applied to reflectron electrodes increases with increasing depth as shown in (Figure 2.4). The ions which have higher energy penetrate deeper in the reflectron array compared to low energy ions. As a result, ions which have same mass but slightly different energies will reach the detector at the same time. MCP is used as a detector in PTR-TOF-MS. MCP is a glass plate containing large no of capillary and arranged in a honeycomb structure and internal surface coated with lead oxide. It amplifies the signal due to arrival of a VOC ion from TOF. When the ion falls on the MCP, it hits the internal surface of the capillary and produces secondary electrons. These electrons collide with the internal surface and emit multiple numbers of electrons. This process

is repeated and finally from one plate about 10^3 electrons are ejected then these 10^3 electrons hit the second MCP plate and produce 10^6 electrons. One ion emits about 10^6 electrons as shown in (Figure 2.5).

2.4 Works done and future plans

1. After joining the SPA-SC Division, I did literature survey about VOCs and their importance in the earth's atmosphere. I have also gone through several review papers to know the present status of VOC based research studies in India and abroad. I learnt the working principle and operational details of PTR-TOF-MS. It is a complex instrument and I am learning more details such as analysis of mass spectrum, calibration and maintenances. I also learned TD-GC-FID instrument, air sampling, calibration, etc. Recently, I am learning the operation of other important supporting systems required for detection of VOCs using both PTR-TOF-MS and TD-GC-FID systems.
2. I have collected air samples in the forested region of the Western Ghats (Bhagwan Mahavir Wildlife Sanctuary). The site is isolated far from the urban area and least affected by anthropogenic emissions. Measurements/Analyses are completed and I am doing data reduction. We are planning to collect more samples to study seasonal variations of BVOCs mixing ratio under different environmental conditions.
3. VOCs in the marine boundary layer of the Arabian Sea: Air samples were collected at different latitude to the latitudinal dependence of BVOCs. We expect, strong latitudinal dependence of BVOCs as distribution of DOC or phytoplankton show strong spatial variation.
4. Estimate the contribution from biogenic and anthropogenic sources: Urban sites are believed to predominantly influenced by anthropogenic emissions. However, VOCs in tropical urban sites are expected to have significant biogenic origin particularly in summer. Thus far, studies in urban sites of India have not considered the variability of BVOCs and related trace



Field Experiments:

1. **Ahmedabad:** Semi Arid Area
2. **Goa:** Tropical evergreen
3. **Arabian Sea:** Oceanic
4. **Dehradun:** Dry Temperate

Figure 2.6: Ongoing and proposed sampling sites/regions in India

constituents. Only anthropogenic emissions have been focused. I have been working to extract data of one-year of measurements using PTR-TOF-MS and TD-GC-FID at Ahmedabad. For several VOCs, originated from both natural and anthropogenic sources, I will study that how contribution from these two types sources vary with season.

5. The branch enclosure experiment will provide an important understanding about the BVOCs emission from an individual plant species. I am working to design a setup for branch enclosure experiment (Figure 2.7). This will help to make a detailed investigation of response to sunlight and temperature.

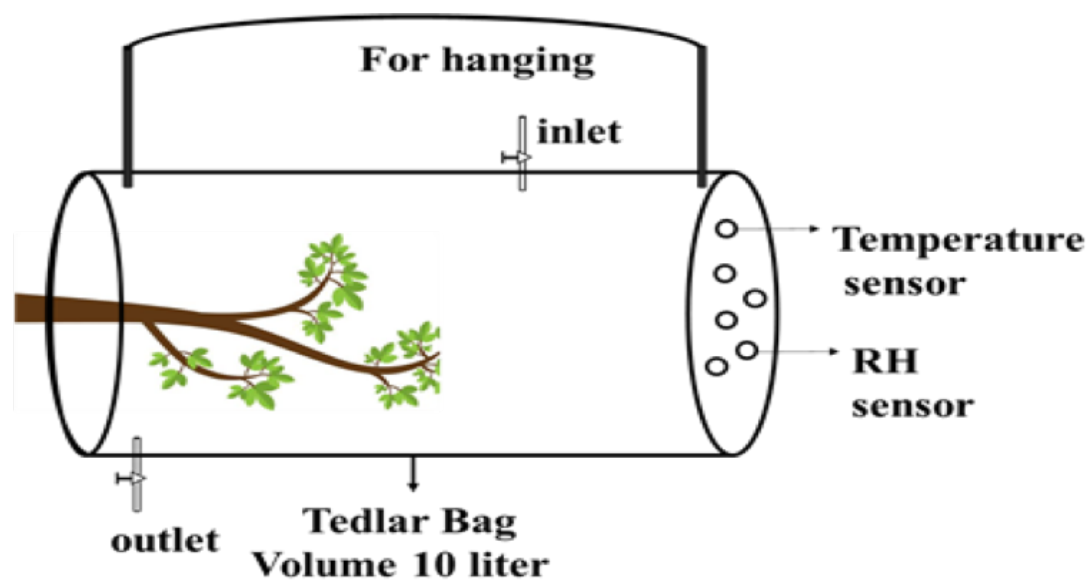


Figure 2.7: Branch enclosure set up diagram

Chapter 3

Elevated levels of biogenic non-methane hydrocarbons in the marine boundary layer

3.1 Introduction

A variety of natural and anthropogenic sources emit volatile organic compounds (VOCs) in the earth's atmosphere. The major sources of natural VOCs, also known as biogenic-VOCs (BVOCs), are emitted from terrestrial vegetation and oceanic biogeochemical constituents [1–6]. Anthropogenic VOCs (AVOCs) are mainly emitted due to the use of fossil fuels, biomass and biofuel burning, and use of chemical solvents. Global emission estimates of BVOCs exceed 1 Pg C yr⁻¹ which is ∼ 10 times larger than that of AVOCs [7, 8]. In the atmosphere, oxidation of VOCs by hydroxyl (OH) radicals can lead to the production of ozone (O³) and secondary organic aerosols (SOA), and therefore indirectly contribute to climate change (Unger, 2014). The fast photo-oxidation of VOCs influences the oxidation capacity of the atmosphere and can affect the lifetime of methane (CH₄) and the production of sulfate and nitrate particles [9–12]. The oceanic emissions of VOC are essential to understand the cloud microphysics and photochemistry in the remote marine atmosphere [13]. About 30% of OH radical concentrations are regulated by their reactions with VOCs in the marine boundary layer (MBL)

[14, 15].

In recent years, several measurement and model based studies have reported the significance of BVOCs emissions from different terrestrial vegetation regions of the world [2]. Thus far, studies over different oceanic regions across the globe have mainly focused to understand the roles of biogeochemical cycles of dimethyl sulfide (DMS), nitrous oxide (N_2O), methane (CH_4) [1, 16, 17]. Although oceanic emissions of VOCs are much smaller than those from terrestrial vegetation but play important role in the atmospheric processes of remote MBL [18, 19]. For example, oceanic emissions are significant sources of many light NMHCs and oxygenated-VOCs (OVOCs) in remote marine regions [20]. The major oceanic NMHCs (e.g., ethane, butane, ethene, propene etc.) belong to functional groups of alkane and alkene [21, 22]. The atmospheric lifetimes of alkenes are about a few days and therefore oceanic emission is an important source in the remote MBL. In addition to oceanic emissions, transport from continental sources contribute to the levels of ethane and propane in the MBL due to their longer atmospheric lifetimes of about a few weeks [23]. Oceanic emissions of NMHCs depend on biological productivity and prevailing meteorological conditions [22]. Therefore, the estimated fluxes of NMHCs from the global ocean are still subject to large uncertainties. In the past few decades, studies on oceanic VOCs are limited mainly over the Atlantic Ocean, Pacific Ocean and smaller basins of Mediterranean Sea, Gulf of Mexico, Black Sea [24–29]. Emissions of NMHCs from the surface seawater show large regional and seasonal variations [30–32]. The global budgets of oceanic alkanes and alkenes have been estimated in the range of $2.5 – 6.0 \text{ Tg C yr}^{-1}$ ([33] and references therein). The dissolved organic carbon (DOC) composed of complex organic compounds represents a major pool of carbon in the upper ocean is an important source of several NMHCs in seawater [22]. The northern Indian Ocean particularly the Arabian Sea is known for high biological productivity in response to the transport of mineral dust from the African continent and Arabian Peninsula [34–36]. Supply of nutrients by upwelling is another important cause of higher productivity of the Arabian Sea during summer monsoon period [37]. The slow-to-degrade DOC produced during the summer monsoon could be a sustain-

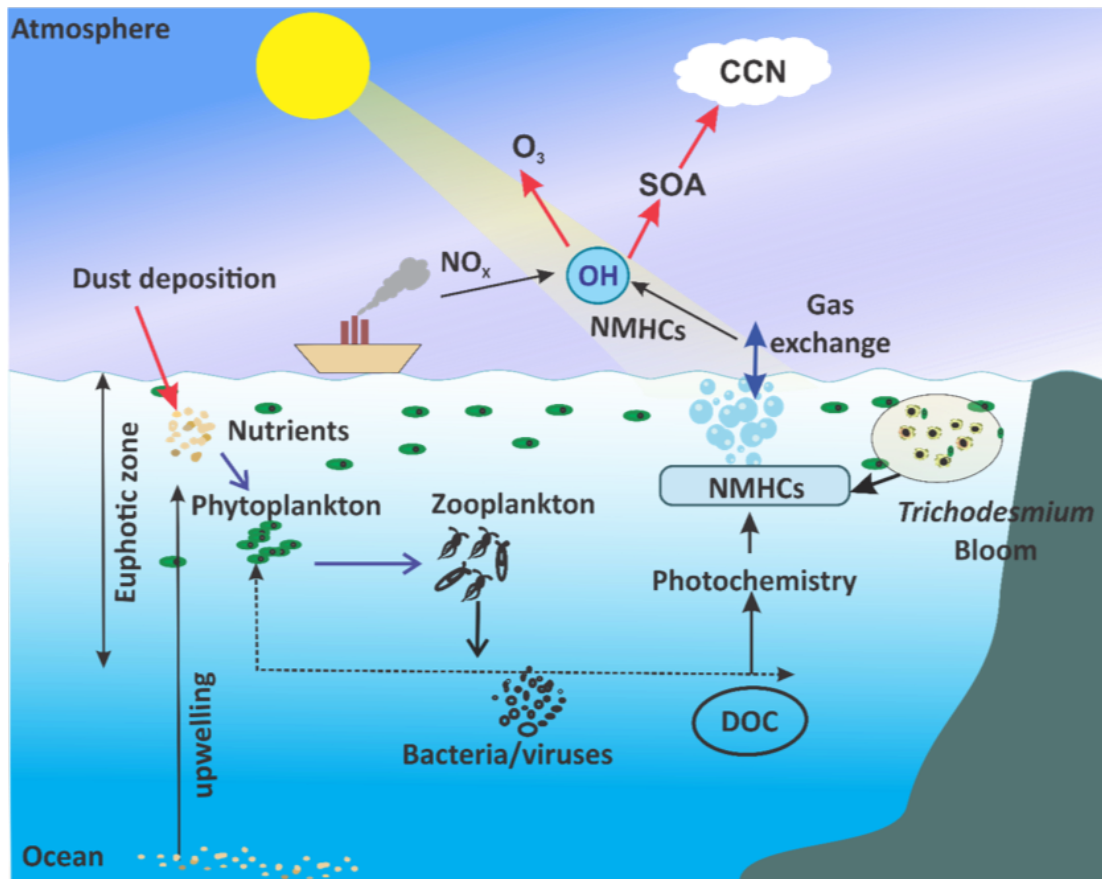


Figure 3.1: Emission from phytoplankton and dissolved organic carbon (DOC) present in ocean water is an important natural source of many non-methane hydrocarbons (NMHCs) in the marine boundary layer (MBL). Phytoplankton takes nutrients from the seawater and zooplankton grazes phytoplankton, and DOC is produced by phytoplankton during photosynthesis. Photo-oxidation of DOC leads to production of NMHCs in seawater. Diatom and cyanobacteria directly produce light NMHCs in the seawater. The exchange of gases from seawater to air is controlled by prevailing meteorological conditions but mainly wind by the wind speed. VOCs released in the marine atmosphere are oxidized by reaction with OH radical and can produce ozone and secondary organic aerosol (SOA) which affect the radiation budget of the earth's atmosphere.

able source of VOCs during pre-summer monsoon [38]. Although the measurements of oceanic VOCs in the MBL of northern Indian Ocean are rare but their emissions from the surface seawater are expected to be very high due to high productivity and favorable tropical conditions. The elevated levels of oceanic VOCs and high anthropogenic emissions of NO_x (= NO + NO₂) mainly from shipping activities could have significant implications on ozone production in the MBL of the Arabian Sea. The shipping emissions of NOx were ~ 5.4 Tg in the year 1950 and have increased to ~ 21.4 Tg in the year 2001 [39]. The average tropospheric ozone concentrations of 2 – 3 Dobson Unit (DU) have been measured over the equatorial to sub-tropical (0 – 45°N) oceanic regions. However, exceptionally high levels of ozone (~ 5 DU) observed over the Persian Gulf and Arabian Sea may be attributed mainly to shipping emissions [40]. The cause of elevated mixing ratios of ozone (> 70 ppbv) measured in the MBL of Arabian Sea during the Indian Ocean Experiment (INDOEX) remains unexplained but roles of photochemical formation and downdraft were speculated [41]. There is, however, no study thus far conducted to understand the role of oceanic NMHCs in the marine boundary layer of Arabian Sea. This study is based on the measurements of oceanic NMHCs in the MBL and biological parameters in surface seawater of the Arabian Sea during pre-monsoon season of the year 2017. The main objective of this campaign was to investigate the distribution, variability and sources of different NMHCs in the MBL covering different productivity regimes. The roles of ocean productivity (phytoplankton and bacteria), sea surface temperature (SST) and other meteorological parameters have discussed to understand the distributions the levels of alkenes in the MBL. A brief comparison with the measurements reported over the Bay of Bengal (BOB) and other oceanic regions of the world has been also presented.

3.2 Campaign and Experimental Methodology

The surface area of the Arabian Sea between latitudes of 0-25 °N and longitudes of 50-80 °E is 6.225×10^6 km² surrounded by the arid land masses of Arabian

Peninsula and Africa in the north and west, by the coastal hills of Western Ghats of India in the east, and by the Indian Ocean in the south [42]. The high productivity and oxygen minimum environments of the Arabian Sea provide unique opportunity to study the climatically induced changes in marine biology and carbon cycle [43]. A cruise campaign onboard Fishery Oceanographic Research Vessel (FORV) Sagar Sampada (Cruise No # SS359) was conducted over the Arabian Sea ($5\text{--}20^{\circ}\text{N}$, $60\text{--}75^{\circ}\text{E}$) from 15 April to 2 May 2017 (Figure -3.2). A total of 50 air samples were collected into the pre-evacuated glass flasks (800–1000 ml) using an oil-free air compressor from the deck of the ship at a height of 15 m above the ocean surface. Air samplings were performed when cruising speeds were around 5–10 knots to avoid possible contaminants from stack emissions. The samples were analyzed for the mixing ratios of C₂-C₆ NMHCs using the thermal desorption (TD) (Unity 2 Markes International GmbH, Germany) coupled with gas chromatography-flame ionization/mass detector (GC-FID/MS, Agilent 7890A) at on shore laboratory at PRL, Ahmedabad within a month of their collection. In the first step, air samples were pre-concentrated on a cold trap (U-T17O3P-2S: Ozone precursors, Markes International GmbH, Germany) at a low temperature of -15°C and then desorbed rapidly by heating at 275°C . The desorbed samples were transferred into the GC column via a heated (100°C) transfer line capillary. The separations of different C₂-C₆ compounds were achieved using an aluminum oxide PLOT (Al₂O₃/Na₂SO₄) column (50 m × 0.53 mm). An ultra-high pure Helium (He) gas (Research Grade 99.9999%, Linde, USA) was used as a carrier gas. The zero air (Parker HPZA-3500-220) and hydrogen (Parker H2PD-300-220) were used as fuel gases for the FID. The high purity nitrogen gas (999.9999%, Parker UHPN2-1100-220) was used as purge gas in the TD and as a make-up gas for the FID. The flow rates of zero air and hydrogen were set at 350 and 35 mL/min, respectively. The GC oven temperature was programmed for the desired separation as follows: initially held at 97°C (0.5 min hold), increased to $110^{\circ}\text{C}/2^{\circ}\text{C min}^{-1}$ (6 min hold), and finally increased to $190^{\circ}\text{C} / 5.2^{\circ}\text{C min}^{-1}$ (10 min hold). The FID signals of different NMHCs were calibrated using a standard mixture containing 1 ppmv of each compound (LE732C 4/15, Linde,

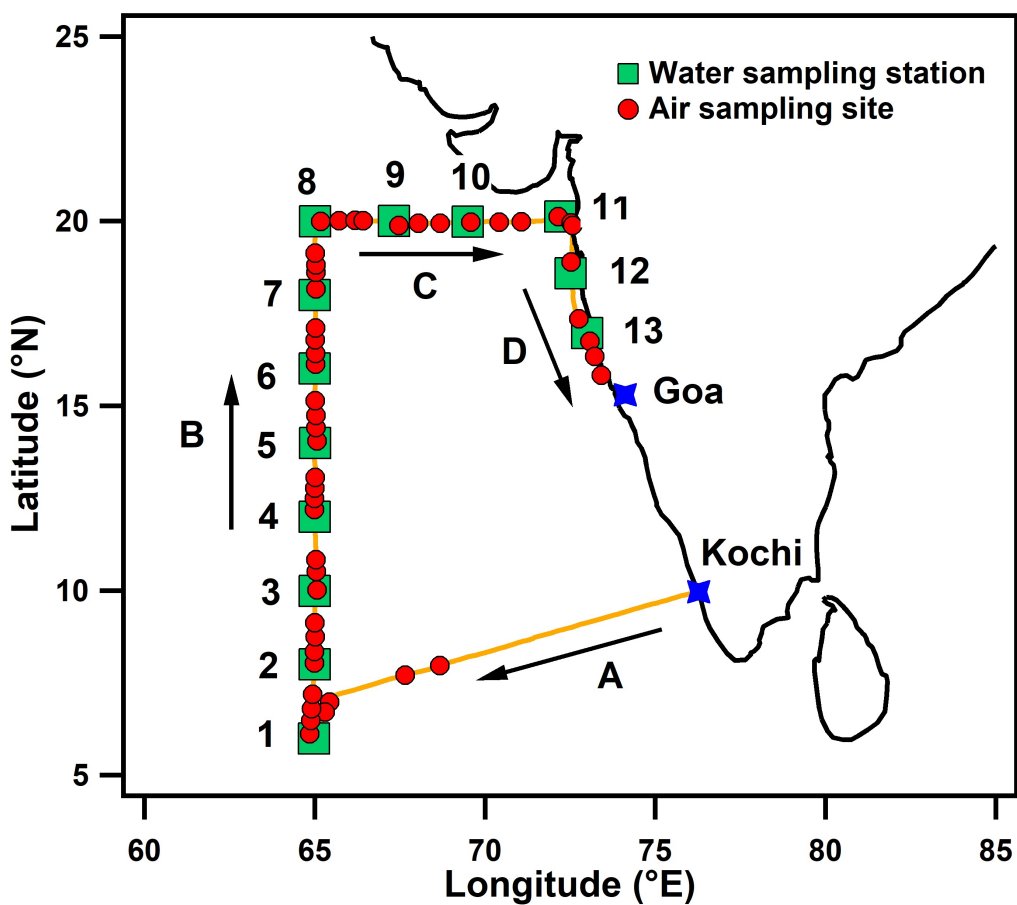


Figure 3.2: Cruise track, different sections (A, B, C and D), air sampling (red circle) and water sampling (green square) locations over the Arabian Sea during 15 April-2 May 2017

USA). The dynamic dilutions of standard mixture at lower concentrations were prepared using a gas calibration unit (GCU-advanced v2.0, Ionicon Analytik). The multipoint calibration curves of different NMHCs used in the present are plotted in Figure-3.9. Figure-3.10 depicts the comparison of chromatograms of NMHCs for air samples collected during the day and night.

Sea water temperature, salinity and pressure were obtained at 13 different stations using onboard CTD rosette sampler. Sea water samples were collected at these stations to estimate chlorophyll-*a* (Chl-*a*) and microscopic counting of ocean microbes. For the analysis of Chl-*a* concentration, water samples (2 L) were gently filtered under low pressure (< 200 mbar) onto Whatman GF/F filters and stored in the dark at -20°C until measurements. At onshore laboratory,

10 mL of 90% acetone was added to these filters. Thereafter, filters were homogenized with glass beads for 5 minutes and centrifuged at 5500 rpm and 0 °C for 10 minutes. The supernatant was removed and the fluorescence was measured using a fluorometer. Water samples were fixed with lugol for microscopic counts. The Hybrid Single Particle Lagrangian Integrated Trajectory (HYSPLIT) 7 days isentropic back trajectories at 100 m above mean sea level (amsl) were calculated to investigate the role of synoptic scale transport [44]. As shown in (Figure 3.3), back trajectory plots at different sampling points are overlaid on monthly mean map of satellite-derived Chl-*a* concentration. The concentration of Chl-*a* is used as an approximately variable for estimating the phytoplankton biomass present in the ocean water. We have used Level 3 Chl-*a* ocean color dataset retrieved from the NASA's Aqua MODIS (Moderate Resolution Imaging Spectro- radiometer) satellite sensor ¹. The monthly mean concentrations of Chl-*a* over the Arabian Sea were in the range of 0 (below detection level) to 1.5 mg m⁻³ during the study period. Localized oceanic emissions of trace gases referred from in-situ or satellite derived Chl-*a* over arbitrary regions may be erroneous without accounting for the transport history of air masses sampled [24]. The meteorological data were measured using the automatic weather system (AWS) installed on the upper deck of the ship. The cruise track has been divided in four sections, i.e. A (15-19 April), B (20-26 April), C (27-30 April) and D (1-2 May). The daily mean air temperature, wind speed and relative humidity (RH) varied in the ranges of 27-31 °C, 1-7 m s⁻¹ and 64-76%, respectively. Statistics of meteorological parameters measured along different sections of the track is presented in Table 3.5. Year 2017 was the warmest year for the global ocean and SST anomalies of greater than 0.5 °C were observed over the Arabian Sea during the study period [45]. The monthly mean SST and wind field reanalysis data were taken from the National Centers for Environmental Prediction (NCEP). The mean SST varies from 27-30 °C over the Arabian Sea (Figure-3.11).

¹(https://neo.sci.gsfc.nasa.gov/view.php?datasetId=MY1DMM_CHLORA)

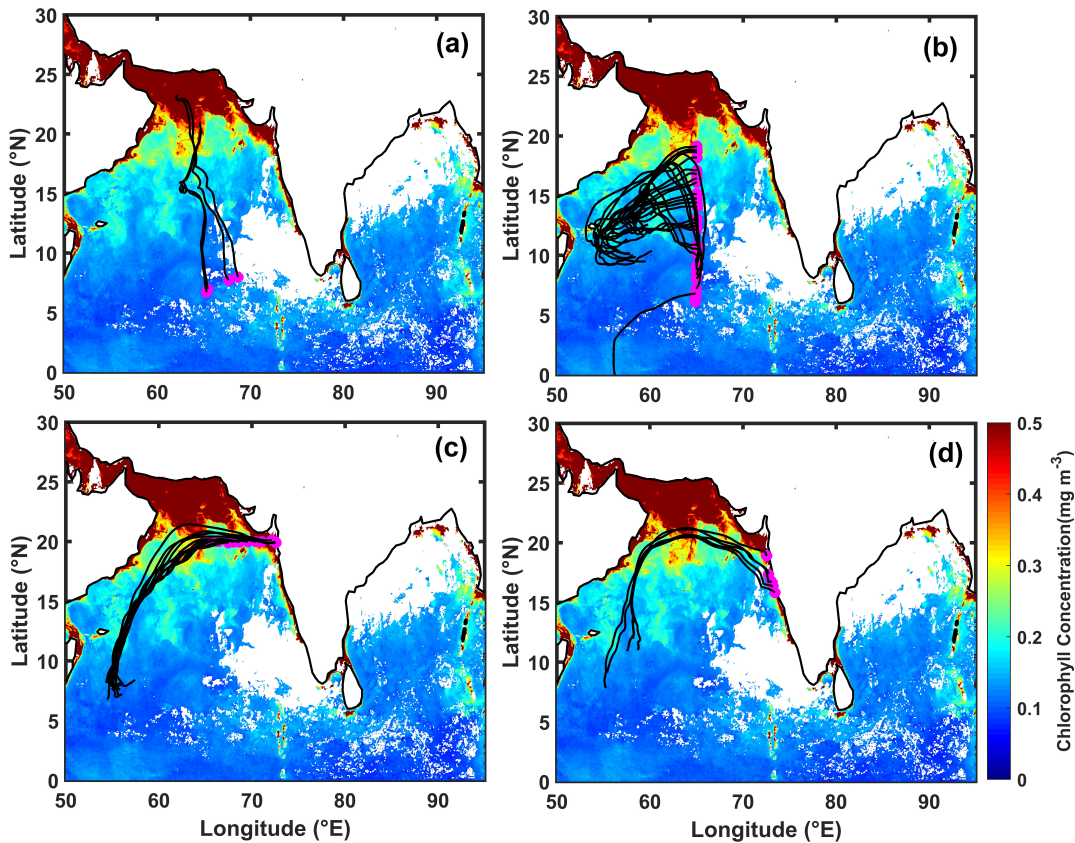


Figure 3.3: 7-day back trajectories at 100 m above mean sea level (amsl) over different air sampling locations.

3.3 Results and Discussion

3.3.1 Time series and diurnal variations of NMHCs

The mixing ratios of ethene, propene, ethane and propane were in the ranges of 1.5-16, 0.6-7, 0.3-4 and 0.08-3 ppbv, respectively throughout the study period (Figure 3.4). The large variations of NMHCs in the MBL were expected as the air samples were collected during both day and night period. The mixing ratio of ethene was highest of 11.37 ± 2.41 ppbv along track A and lowest of 7.55 ± 3.87 along the track B. On an average, the mixing ratios of ethene were 2-3 times higher than those of propene which is consistent with their productions from DOC in the ocean water [6]. The higher mixing ratios of alkenes were due to the higher abundances of *Trichodesmium* (a diazotrophic cyanobacteria) measured over the southern (A) and northern (C) regions. [46] reported higher abundances of Tri-

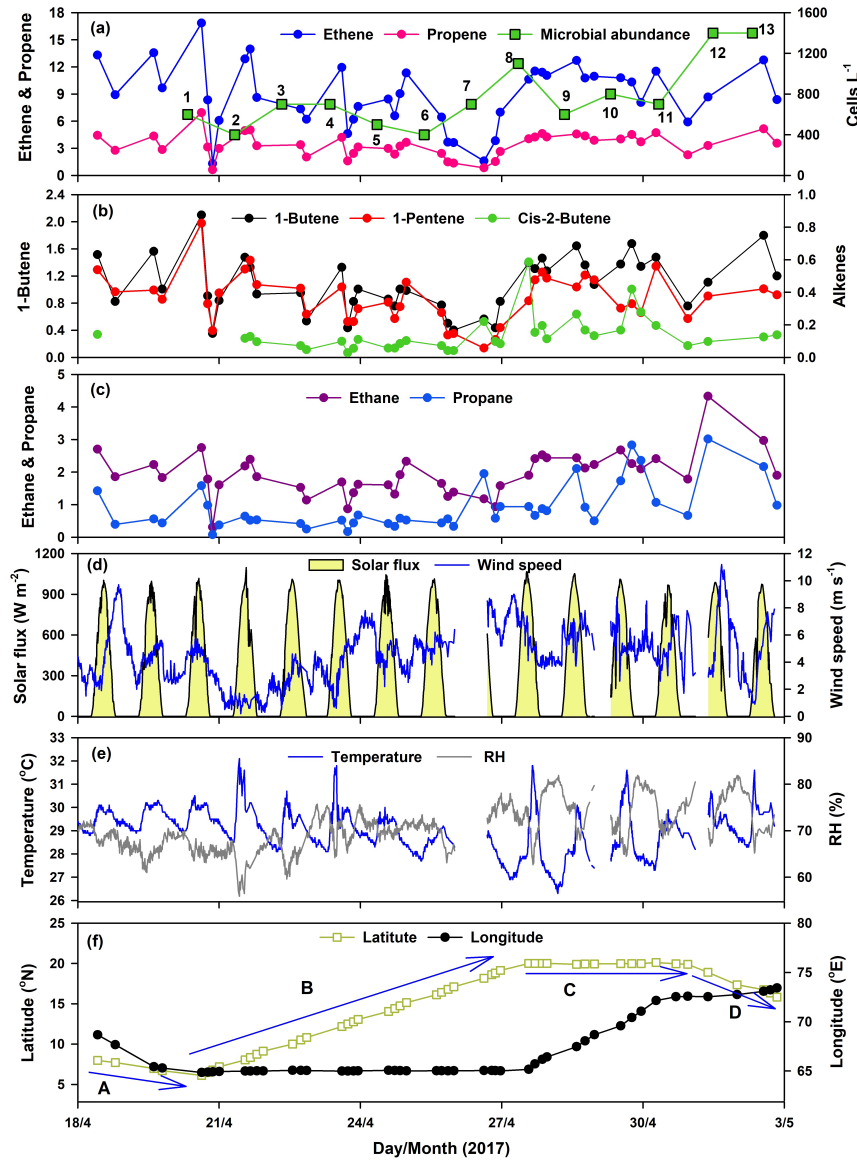


Figure 3.4: Time series of the mixing ratios (ppbv) of (a) ethene, propene and total (sum of 100 different diatom species measured at 1-13 stations), (b) 1-butene, 1-pentene and Cis-2-butane (c) ethane and propane, (d) solar radiation flux and relative humidity, (e) ambient temperature and wind speed and (f) latitude and longitude of air sampling locations along the cruise track

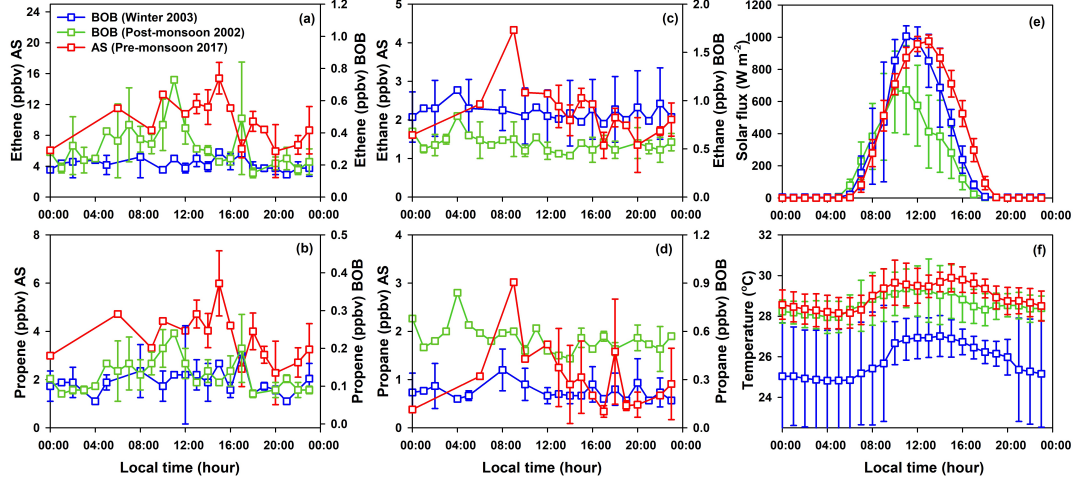


Figure 3.5: Average diurnal patterns of NMHCs mixing ratio, solar flux and ambient temperature over the Arabian Sea during 15 April-2 May 2017. The diurnal dependencies of NMHCs and meteorological parameters measured over the Bay of Bengal during monsoon/post-monsoon (BOB 2002) and winter (BOB 2003) seasons are also plotted for the comparison. Bay of Bengal data are taken from Sahu et al., (2010).

chodesmium in the seawater over the southern Arabian Sea during oligotrophic (low nutrients) conditions which is consistent with our microscopic observations (Table 3.5). The high abundances of Trichodesmium and Rhizosolenia were also reported in the southwest Indian Ocean during the austral bloom [47] and in the southeastern Arabian Sea (SEAS) during pre-monsoon season [48, 49]. The cell densities of 97 different species of diatom and cyanobacteria measured at 13 different stations are shown in (Figure 3.4c). The major diatom and cyanobacteria responsible for the production of alkene in seawater are presented in Table 3.5. Significant productions of alkenes from Trichodesmium colonies in the oligotrophic region of subtropical North Pacific Ocean were reported by [50].

The mixing ratios of both ethene and propene over the central region (track B) show larger variability compared to other regions of the Arabian Sea (Table 3.5). On 20 April at 15:00 local time (LT), the highest mixing ratios of ethene (16.85 ppbv) and propene (6.95 ppbv) coincide with the stronger winds ($> 4 \text{ m s}^{-1}$) from NW, higher temperature ($> 30^\circ\text{C}$) and intense solar radiation ($\sim 789 \text{ W}$

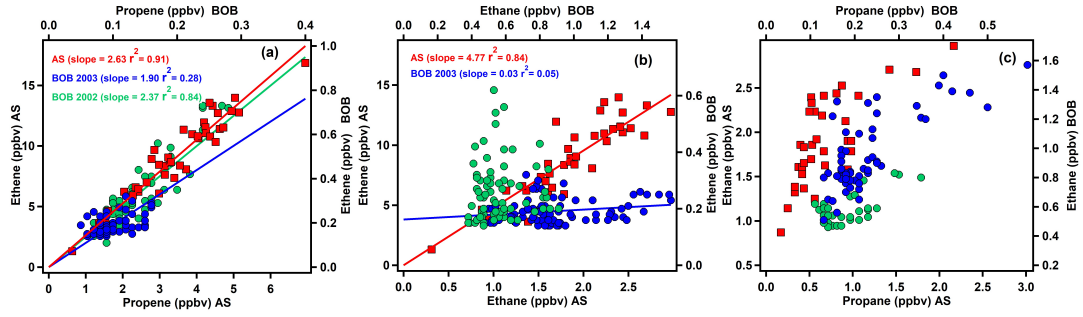


Figure 3.6: Scatter plots of (a) ethene versus propene, (b) ethene versus ethane and (c) ethane versus propane measured during the present study, BOB 2002 and BOB 2003 campaigns

m^{-2}). On the contrary, the lowest values of alkenes in the night (21:00 LT) of 20 April coincided with the low winds ($<3 \text{ m s}^{-1}$) from the west. The time series of alkanes (ethane and propane) show similar trends to those of alkenes but mainly over the central Arabian Sea (Figure 3.5). Air samples were collected during both day and night and this seems to be one of the factors for large variations of NMHCs in the MBL. The air-sea gas exchange is controlled by several parameters such as ocean productivity, solar radiation flux, SST and wind speed which show strong diurnal dependence [51, 52]. Average diurnal mixing ratios of NMHCs and meteorological parameters are plotted to investigate their local time dependence in the MBL (Figure 3.5). However, there is a lack of data for early morning hours (00:00-06:00 LT) as very few samples were collected during this period of the day. The mixing ratios of alkenes were particularly elevated in the afternoon hours, while relatively lower values were observed during evening and night hours (18:00-24:00 LT). To some extent, the diurnal pattern of alkenes seems to follow the diurnal cycles of solar flux and temperature. The daytime average mixing ratios of the ethene ($10.17 \pm 3.66 \text{ ppbv}$) and propene ($3.83 \pm 1.38 \text{ ppbv}$) are $\sim 20\%$ higher than their nighttime values of $8.00 \pm 3.08 \text{ ppbv}$ and $3.07 \pm 1.18 \text{ ppbv}$, respectively (Table 3.5). Ethane and propane showed slightly higher values in the daytime but the overall diurnal patterns are less pronounced than those of alkenes.

The BOB is the eastern basin of the northern Indian Ocean where climatic

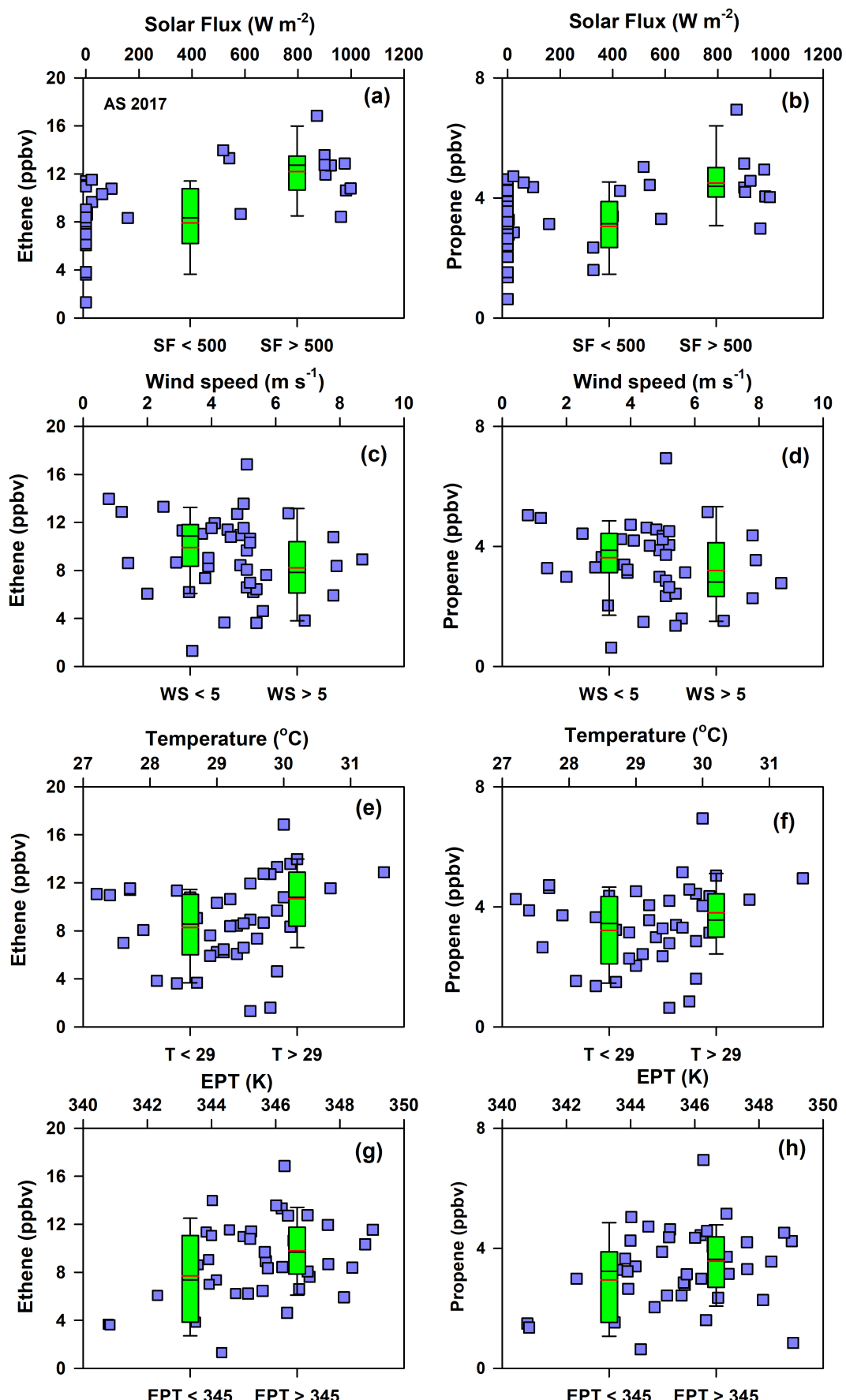


Figure 3.7: The relations of ethene and propene with (a, b) solar flux, (c, d) wind speed, (e, f) temperature and (g, h) equivalent potential temperature (EPT).

The Box-whiskers represent statistics of ethene and propene for higher and lower

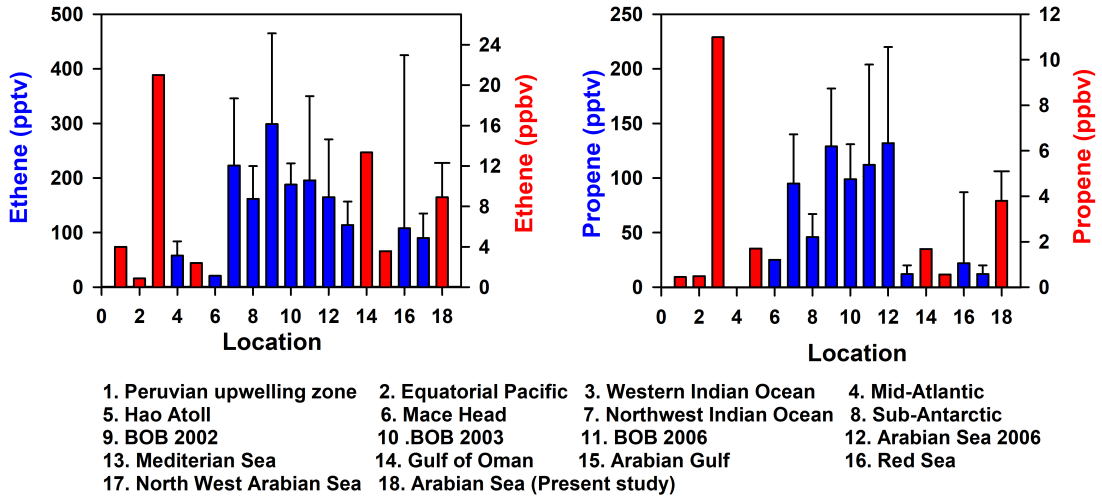


Figure 3.8: Comparison with the mixing ratios of ethene and propene measured in the marine boundary layer (MBL) of different oceanic regions of world. Further details of the data and references are given in Table S1.

conditions are similar to that of the Arabian Sea. The BOB is biologically less productive compared to the Arabian Sea and comparison of NMHCs measured in the MBL of these two basins will highlight the significance of ocean sources. The average diurnal mixing ratios of NMHCs and meteorological parameters measured in the MBL of BOB during the monsoon/post-monsoon of the year 2002 (BOB 2002) and winter season of the year 2003 (BOB 2003) are compared in (Figure-3.5) [52]. The levels of NMHCs in the present study are much higher than their concentrations measured over the BOB during both the seasons. The diurnal maxima of ethene were ~ 13 , 0.6 and 0.3 ppbv during the Arabian Sea 2017 (present study), BOB 2002 and BOB 2003 campaigns, respectively. The intensities of solar flux during the present study are comparable but the values of ambient temperature were 2-3 °C higher than those measured during the BOB 2003. On the other hand, the values of ambient temperature during the present study were almost same to those measured during the post-monsoon BOB 2002. The rather small differences in the values of key meteorological parameters cannot explain the much higher levels of NMHCs observed over the Arabian Sea. Therefore, it is important to compare the biological productions of DOC in seawater

and DOC and air-sea in these two basins of the northern Indian Ocean.

The mixing ratios of ethene and propene measured in the MBL of different oceanic regions of the world show strong diurnal dependence (e.g., Lewis et al., 1999; Ratte et al., 1993; Rudolph & Johnen, 1990). Measurements of alkenes in marine air masses at the coastal sites of Cape Grim, Tasmania and Mace Head, Ireland exhibited maximum levels during the noon hours (Lewis et al., 1999). The higher daytime emissions of alkenes from the equatorial oceans reflected in their greater daytime mixing ratios in the adjacent MBL (Bonsang et al., 2008). A more quantitative description of the diurnal dependence of NMHCs in the MBL needs to consider the strong spatial and day-to-day variations of DOC, SST and meteorological parameters.

3.3.2 Latitudinal variation of NMHCs

One of the objectives of this study was to investigate the variation of NMHCs particularly in view of the latitudinal changes in ocean productivity and meteorological conditions. As shown in Figure-3.12, the mixing ratios of alkenes and alkanes do not show any clear latitudinal dependence (6-20 °N, along 65 °E). The large variability of alkenes could be due to significant variations in DOC, SST and meteorological parameters. As inferred from solar flux data, the intermittent high and low values of alkenes were due to their measurements during day and night hours, respectively. In the southern Arabia Sea at around 6-7 °N, the elevated levels of alkenes coincide with the higher temperatures, presence of *Trichodesmium* and transport from highly productive region of the Gulf of Oman (Figure 2). At lower latitudes, emissions of alkenes seem to be very sensitive to solar flux and SST leading to significant differences between day and night values. The elevated levels of alkenes over the northern Arabian Sea (~20 °N, 65-73 °E) and coastal region were due to high local productivity as inferred from the concentrations of Chl-*a* and cyanobacteria (Figure 3.3). In addition to local emissions, the back trajectories over the northern and coastal regions suggest transport of air masses from highly productive regions of western Arabian Sea.

The oceanic mixed layer is supersaturated by more than an order of magnitude

for most light NMHCs relative to the atmosphere (Plass-Dülmer et al., 1993). The loss of NMHCs from the surface seawater occurs due to sea-air transfer, microbial consumption, aqueous chemistry and physical mixing or dilution (Riemer et al., 2000). The air-sea exchange of trace gases can be determined by the following equation (Unger et al., 2003).

$$F = k_t \left(C_w - \frac{C_\alpha}{\alpha} \right) \quad (3.1)$$

Where F is the flux of a trace gas, k_t is the transfer velocity, C_w is the concentration in water, C_α is the concentration in air and α is the liquid over gas solubility constant (Kim et al., 2017). The C_w of NMHCs strongly depends on the concentration of DOC and intensity of solar radiation. The concentrations of several NMHCs including alkenes in seawater of the western Indian Ocean are reported to be 2-3 times greater than those measured in air (Bonsang et al., 1988). The transfer velocity depends on several meteorological parameters, but mainly on wind speed and temperature (Liss & Merlivat, 1986). Therefore, the latitudinal variations of NMHCs in

the MBL are mainly controlled by the distribution of DOC and meteorological field. The satellite-based ocean color map shows much higher productivity in the northern and coastal regions compared to the central Arabian Sea supporting the large spatial and temporal variations of alkenes in the MBL. In the present study, the mixing ratios of ethene and propene showed a strong correlation ($r^2=0.92$) and a slope ($\Delta\text{ethene}/\Delta\text{propene}$) of $2.62 \text{ ppb ppb}^{-1}$ (Figure 3.6). Although the levels of alkenes over BOB were significantly low but they also showed similar strong relations ($r^2= 0.82$, $\Delta\text{ethene}/\Delta\text{propene} = 2.32 \text{ ppb ppb}^{-1}$). The ethene/propene ratios of $\sim 2.2 \pm 0.6 \text{ ppb ppb}^{-1}$ in the MBL were estimated from the data measured over different oceanic regions of the world (Niki & Becker, 2013). The ratios of ethene/propene measured in the MBL of the northern India Ocean fall within the range of values reported for several other oceanic regions confirming the similar production mechanisms of alkenes in the global seawater. The mixing ratios of 1-butene and 1-pentene also showed tight correlation ($r^2 \approx 0.80$) with ethene suggesting oceanic emissions of other alkenes. As shown in (Figure-3.6b), ethane showed strong correlation ($r^2 = 0.84$) with

ethene which indicates oceanic emissions of alkanes as well. Several studies have reported that oceanic emissions can be a significant source of alkanes in the MBL. The ratios of ethane/propane were between 1.2-1.9 ppb ppb⁻¹ during the major enhancements of alkenes. Typically, the ratios of ethane/propane in the MBL were measured to be in the range of 1.2 – 3.7 ppb ppb⁻¹(Broadgate et al., 1997; Plass-Dülmer et al., 1993; Plass-Dülmer et al., 1995).

3.3.3 Role of ocean productivity

The presence of light NMHCs in seawater with high concentrations of ethene and propene was first reported by Swinnerton and Linnenbom (1967). The average concentrations of ethene and propene in the tropical ocean water were about 4.8 and 1.4 nL L⁻¹, respectively (Swinnerton & Lamontagne, 1974). Ratte et al. (1995) reported significant productions of NMHCs in seawater and found relations with the biological activities in the culture experiments. The production mechanism of alkenes from DOC was first proposed by Wilson et al. (1970). In addition to DOC, diatoms such as *Chaetoceros* and *Thalassiosira* also produce ethene and propene in the exposure of sunlight (Wilson et al., 1970; Ratte et al., 1993). In this study, presence of *Thalassiosira* was measured in the seawater at four water sampling stations (9, 10, 11 and 12). The presence of diatoms including *Nitzschia*, *Thalassiosira* and *Gymnodiniu* in the surface seawater of the northern and coastal Arabian Sea could have caused high mixing ratios of alkenes in the MBL (Table 3). These diatoms are also known to produce ethene and propene in the ocean water (Ratte et al., 1993). Alkenes are also produced by *Trichodesmium cyanobacterium* under high light conditions while undergoing photosynthesis. The annual cycle of DOC stocks in the Arabian Sea showed lowest concentration during the late southwest (SW) monsoon and highest during winter to pre-monsoon period (Hansell, 2009). The higher concentrations of DOC, blooms of diatom, intense solar radiation and high SST during the pre-monsoon season could enhance the production and sea-air exchange of biogenic NMHCs into the MBL.

3.3.4 Dependence of NMHCs on meteorological parameters

The mixing ratios of NMHCs were relatively high during the periods of high solar flux, temperature and wind speed (Figure 3.4). The production of alkenes in seawater depends on the DOC concentration and light attenuation (Bonsang et al., 2008). Alkenes are produced in the presence of sunlight while their concentrations remain constant in the dark (Ratte et al., 1993). The elevated mixing ratios of ethene (12 ± 4 ppbv) and propene (4 ± 1 ppbv) were measured under higher solar irradiation ($>500 \text{ W m}^{-2}$), whereas the values were low at lower solar fluxes ($<500 \text{ W m}^{-2}$) (Figures 3.7a and 3.7b). Although the levels of both ethene and propene were much low compared to the present study but showed similar dependence with solar flux during the BOB 2002 campaign (Figure-??). But the measurements in the winter season during BOB 2003 did not show significant relations of alkenes with the solar flux (Figure S6).

As shown in (Figures 3.7c and 3.7d), the values of alkenes in high wind speed regimes ($> 5 \text{ m s}^{-1}$) were lower than those measured in low and moderate wind speed regimes ($< 5 \text{ m s}^{-1}$). This suggests that the lower values of alkenes were predominantly the result of oceanic emissions and dilution of these emissions by stronger winds from higher altitudes. Also, large patches of *Trichodesmium* blooms were observed during the low wind speeds over the NE and central Arabian Sea in the pre-monsoon period (Capone et al., 1998; Gandhi et al., 2011). The calm sea, high solar flux, warm water and high salinity provide favorable conditions for proliferation for *Trichodesmium* blooms (Devassy et al., 1978). Matondkar et al. (2006) have reported thick blooms of *Trichodesmium* over the Arabian Sea under lower wind speeds ($< 4 \text{ m s}^{-1}$). The higher concentrations of ethene in seawater were observed during calm sunny condition (Ratte et al., 1995). However, the levels of alkenes in the MBL of the Bay of Bengal increased with the increasing wind speed during the BOB 2002 campaign (Figure S5). In the winter season, the measurements of alkenes did not show any relation with the wind speed during BOB 2003 (Figure S6). These distinct relations of alkenes with wind speed can be expected due to the higher biological productivity of the

Arabian Sea compared to less productive BOB.

The ranges of air temperature and SST were rather small to comprehensively investigate their impacts in the concentrations of NMHCs in the MBL. Nonetheless, the mixing ratios of ethene and propene showed slightly higher values at higher air temperatures ($>30^{\circ}\text{C}$) than those observed at relatively lower temperatures ($<30^{\circ}\text{C}$) (Figures 3.7e and 3.7f). Unlike the present study, the relations of alkenes with air temperature over the Bay of Bengal during BOB 2002 and BOB 2003 did not show any clear dependence with temperature (Figure-?? and S6). The equivalent potential temperature (EPT, θ_e) which is a conserved quantity is a better parameter to investigate the impact of fresh oceanic emissions. The EPT can be derived using following equation (Sahu et al., 2013).

$$\theta_e = \left(T + \frac{L_v q}{C_{pd}} \right) \times \left(\frac{P_0}{P} \right)^{R_d/C_{pd}}. \quad (3.2)$$

Where, P and T are pressure (hPa) and temperature (K) of air parcel, respectively. R_d is gas constant for dry air ($287.04 \text{ J kg}^{-1}\text{K}^{-1}$) and C_{pd} is the specific heat capacity at constant pressure ($1005.7 \text{ J kg}^{-1} \text{ K}^{-1}$). q and L_v are the specific humidity (g kg^{-1}) and latent heat of water vapor, respectively. P_0 is the standard pressure (1000 hPa). The values of θ_e varied in the range of 340-350 K during the campaign. Typically, the higher and lower values of θ_e represent fresh oceanic emissions and aged atmospheric air related to the updraft and downdraft motions, respectively. Therefore, higher levels of alkenes measured at higher θ_e ($>345 \text{ K}$) indicate the influence of fresh oceanic air masses (Figures 3.7g and 3.7h).

3.4 Comparison with other oceanic regions

We have compared the maximum mixing ratios of light alkenes measured in the MBL of different oceanic regions of the world with the present study (Figure 3.8). As summarized in Table S1, the mixing ratios of ethene and propene over the Arabian Sea measured are much higher compared to a large range of values reported over most of the oceanic regions of the world. The higher levels of ethene and propene were reported in the MBL of a few productive marine regions such as

the western Indian Ocean and Gulf of Oman. Bonsang et al. (1988) have reported very high levels of ethene (0.8-21 ppbv) and propene (2.5-15 ppbv) over the inter-tropical Indian Ocean (25 °S -13 °N) in April 1985. In a recent study, high levels of ethene (propene) 13.3 (1.7 ppbv) and 3.6 (0.56 ppbv) are reported over the Gulf of Oman and Arabian Gulf, respectively (Bourtsoukidis et al., 2019). In the late spring season, high levels of ethene (\sim 4 ppbv) and propene (\sim 4.5 ppbv) were observed over Hao atoll, southern Pacific Ocean (Bonsang et al., 1992). Typically, the levels of alkenes measured in the present study are comparable to the values reported for tropical oceans (Bonsang et al., 1988; Greenberg & Zimmerman, 1984). Ogawa & Tanoue, (2003) have reported the DOC concentrations measured over the different oceanic regions of world. The concentrations of DOC in the surface seawaters of mid Atlantic Ocean, Pacific Ocean and Arabian Sea were 70-80 and 60-80 and 65-95 μ M, respectively (Ogawa & Tanoue, 2003). The Peruvian upwelling region is also an anoxic marine zones (AMZs) like the Arabian Sea (Ulloa et al., 2012). Therefore, in these regions the higher productivity could be one of the reasons for higher values of alkenes and alkanes in the marine air. Overall, the large variations in the concentrations of light alkenes in the global MBL could be due to their significant spatio-temporal dependence in the governing parameters such DOC, SST, solar flux and prevailing meteorological conditions. The highest concentrations of oceanic NMHCs in the MBL of different oceanic regions were measured during the spring and summer seasons. This could be at least partially due to enhanced marine biological activity for these seasons.

3.5 Conclusion

The Arabian Sea is one of the most biologically productive oceanic regions of the world where measurements of VOCs in seawater and marine boundary layer are scarce. Measurements of different NMHCs in marine air samples were performed over the Arabian Sea during a cruise campaign in the pre-monsoon season of the year 2017. The mixing ratios of NMHCs were relatively high and showed large spatiotemporal variations. Light alkenes were the dominant species throughout

the study period. Levels of NMHCs over the northern and coastal regions were 40% higher than those measured over the central Arabian Sea. Phytoplankton abundance played important role in the distributions of oceanic NMHCs in the MBL. The presence of diatoms and cyanobacteria such as *Thalassiosira* and *Trichodesmium* in seawater and high SST ($>28^{\circ}\text{C}$) greatly enhanced the production of alkenes and other oceanic hydrocarbons. Overall, physical and biological processes in surface seawater and the prevailing meteorological conditions influenced the sea-air exchange of NMHCs. In addition to localized oceanic emissions, transport of air masses mainly from the more productive regions of western and northern Arabian Sea was another reason for the large latitudinal variations of NMHCs. The mixing ratios of alkenes showed significant diurnal variations as their daytime values were 20% higher than the nighttime values. A strong positive correlation between different alkenes along with the ethene/propene ratios of $\sim 2.2 \pm 0.6 \text{ ppb ppb}^{-1}$ (which fall in the range reported for several oceanic regions) confirms their similar production mechanisms to those in the global ocean water. The mean levels of both ethene and propene were significantly higher than those reported for other oceanic regions of the world. The mixing ratios of ethene and propene observed during the present study were 15-20 times higher than their levels measured over the Bay of Bengal during the monsoon/post-monsoon and winter seasons. The high atmospheric concentrations of NMHCs could be one of the reasons for the elevated tropospheric ozone reported in the MBL of the Arabian Sea. A comprehensive study is required to understand the role of biogeochemical processes controlling production of NMHCs in seawater and their sea-air exchange over the northern Indian Ocean.

List of Tables

Table 3.1: The average \pm standard deviation of the mixing ratios of NMHCs (ppbv) and meteorological parameters measured along four different tracks over the Arabian Sea during 15 April-2 May 2017.

Compound/Parameter	Track A	Track B	Track C	Track D
Ethane	2.16 \pm 0.41	1.58 \pm 0.54	2.28 \pm 0.26	3.07 \pm 1.22
Ethene	11.37 \pm 2.41	7.55 \pm 3.87	10.48 \pm 1.80	9.94 \pm 2.45
Propane	0.71 \pm 0.49	0.60 \pm 0.43	1.29 \pm 0.77	2.06 \pm 1.02
Propene	3.61 \pm 0.91	2.88 \pm 1.46	4.10 \pm 0.65	4.00 \pm 1.00
1-butene	1.23 \pm 0.37	0.88 \pm 0.40	1.35 \pm 0.24	1.37 \pm 0.37
cis-2-butene	0.14	0.09 \pm 0.04	0.23 \pm 0.14	0.12 \pm 0.02
1-pentene	0.43 \pm 0.08	0.32 \pm 0.18	0.41 \pm 0.11	0.39 \pm 0.02
Wind speed (m s ⁻¹)	4.26 \pm 1.44	4.07 \pm 1.94	5.47 \pm 0.41	5.24 \pm 2.23
Temp (°C)	30.17 \pm 1.01	28.98 \pm 0.53	28.31 \pm 0.56	29.28 \pm 0.18
RH (%)	69 \pm 2	69 \pm 3	75 \pm 2	75 \pm 0.47
Pressure (hPa)	1008 \pm 1.57	1009 \pm 0.45	1009 \pm 0.83	1008 \pm 0.56

Table 3.2: The average \pm standard deviation of the mixing ratios of NMHCs (ppbv) measured over open ocean and coastal regions, and for daytime and nighttime over the Arabian Sea.

Species	Open ocean	Coastal	Daytime	Nighttime
Ethane	1.67 \pm 0.57	2.38 \pm 0.63	2.14 \pm 0.77	1.80 \pm 0.59
Ethene	8.16 \pm 4.00	10.16 \pm 2.00	10.17 \pm 3.66	8.00 \pm 3.05
Propane	0.61 \pm 0.43	1.41 \pm 0.83	1.17 \pm 0.87	0.74 \pm 0.54
Propene	3.00 \pm 1.43	4.00 \pm 0.76	3.83 \pm 1.38	3.07 \pm 1.18
1-Butene	0.93 \pm 0.42	1.32 \pm 0.28	1.24 \pm 0.43	0.97 \pm 0.38
cis-2-Butene	0.09 \pm 0.05	0.2 \pm 0.13	0.17 \pm 0.14	0.12 \pm 0.06
1-Pentene	0.34 \pm 0.17	0.40 \pm 0.11	0.40 \pm 0.16	0.34 \pm 0.14

Table 3.3: List of water sampling stations where abundance of diatom and cyanobacteria community (cells L-1) was measured which are known to contribute the production of ethene and propene in the seawater (Ratte et al., 1993)

Station	Date	Lat (° N)	Long (° E)	Nitzschia	Thalassiosira	Gymnodinium	Trichodesmium	Ethene (ppbv)	Propene (ppbv)
1	20-Apr	6	65	0	0	0	500	16.85	6.94
2	21-Apr	8	65	0	0	0	0	12.88	4.95
3	22-Apr	10	65	0	0	0	0	-	-
4	23-Apr	12	65	0	0	0	0	11.94	4.2
5	24-Apr	14	65	0	200	0	0	8.44	2.99
6	25-Apr	16	65	0	200	0	0	-	-
7	26-Apr	18	65	0	0	100	0	1.6	0.84
8	27-Apr	20	65	0	0	100	0	10.63	4.05
9	28-Apr	20	67.3	0	200	100	0	12.71	4.57
10	29-Apr	20	69.5	100	300	0	0	10.79	4.03
11	30-Apr	20.1	72.2	100	300	0	0	11.52	4.72
12	1-May	18.6	72.5	0	400	200	0	8.67	3.31
13	2-May	17	73	0	0	0	1200	12.76	5.15

Supplementary Tables and Figures

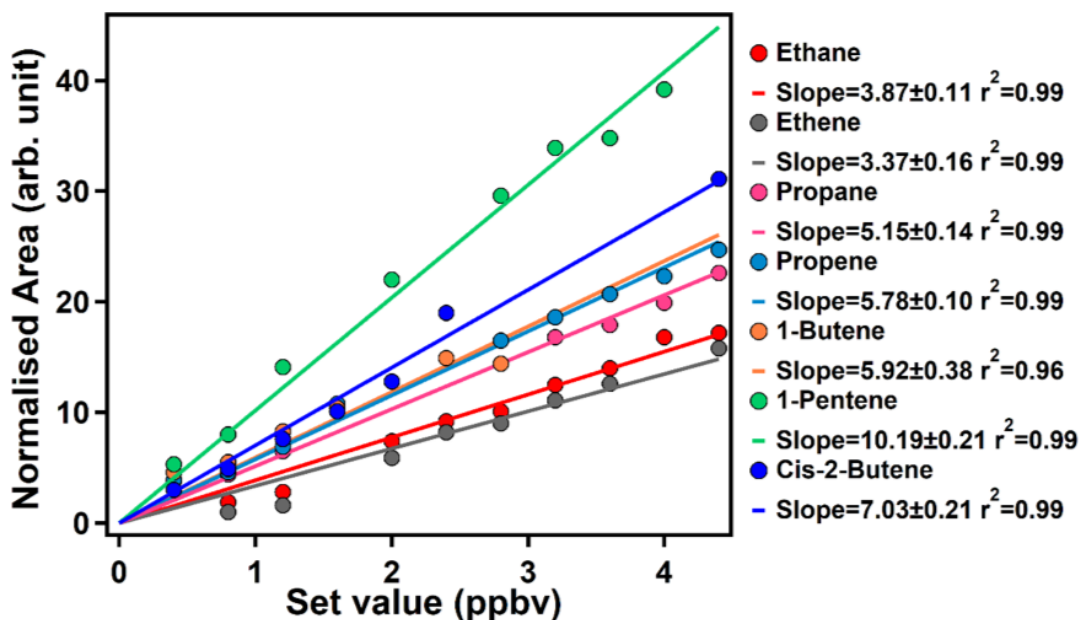


Figure 3.9: Calibration plot of NMHCs. All the above set values of NMHCs are showing good relationships with area under curve.

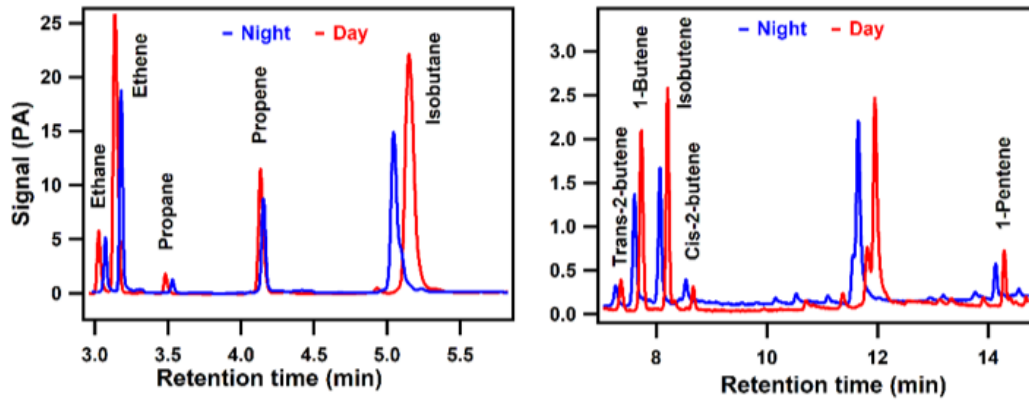


Figure 3.10: Chromatograms of the VOCs analyzed by TD-GC-FID for air samples collected during the day and night. The amplitude and area under the peaks of alkene during daytime were greater than those for nighttime.

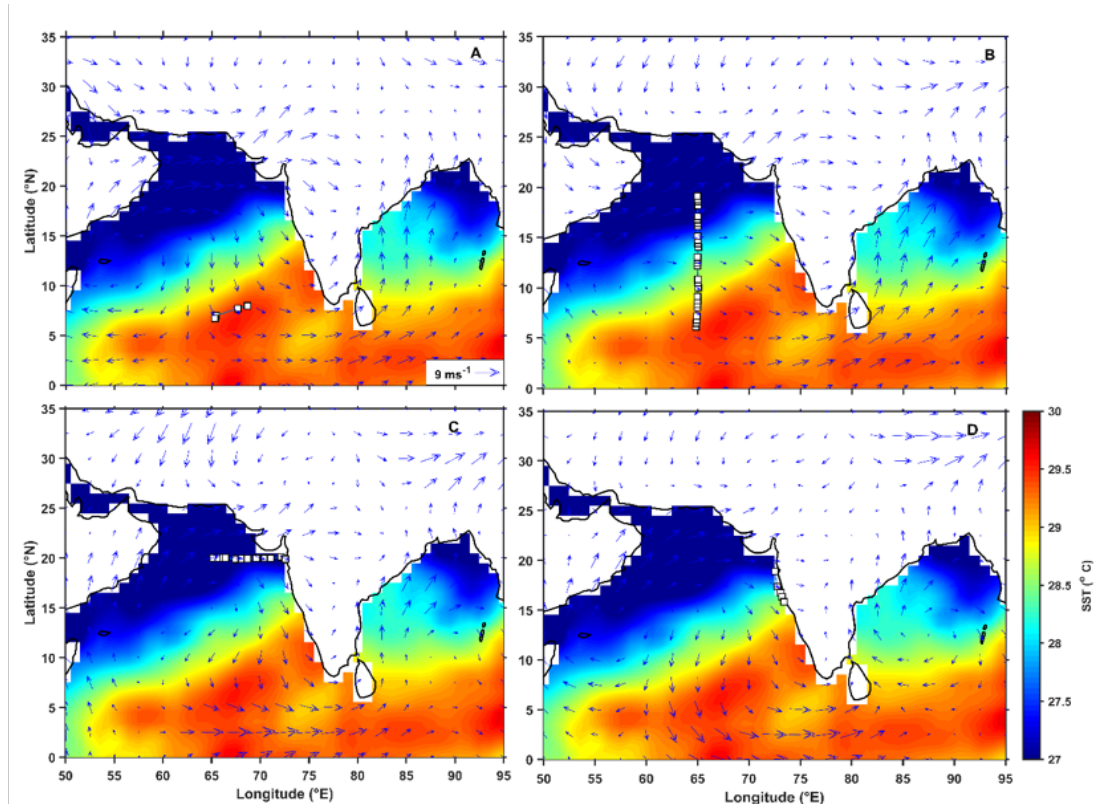


Figure 3.11: Average wind stream line at 1000 hpa pressure level and sea surface temperature (SST) during April using NCEP data over the Arabian sea for different cruise track A, B, C and D. For cruise track A, the flow of wind is from the north (higher productive region) which also contribute to high mixing ratios of alkenes.

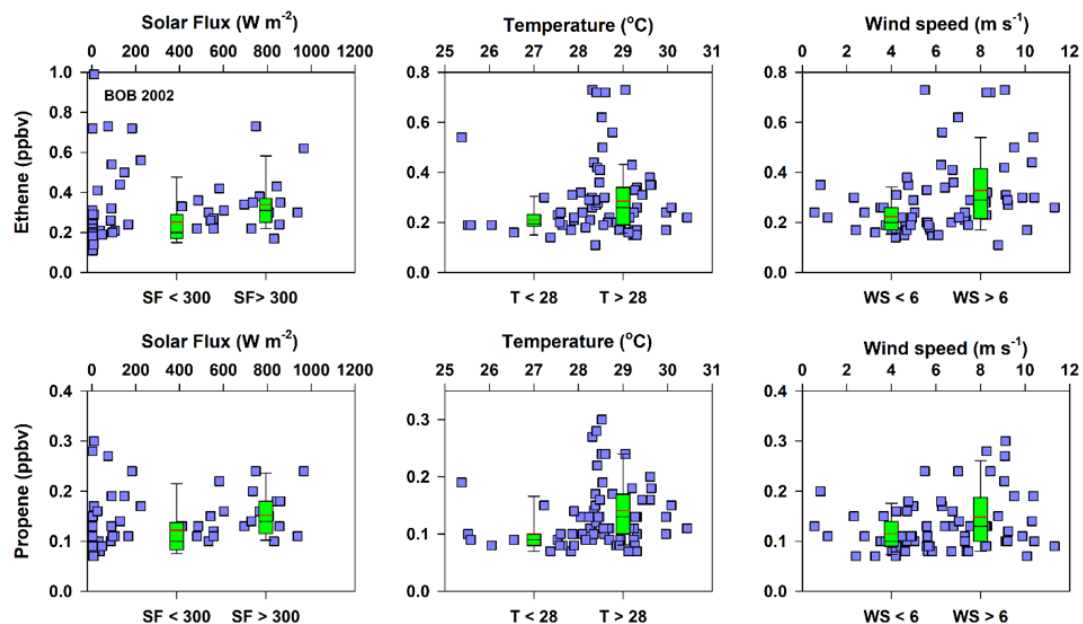


Figure 3.12: The box whisker plots show that the mean value of ethene and propene with solar flux, temperature and wind speed over the Bay of Bengal during post-monsoon (September-October) BOB 2002 campaign. Here solar flux, ambient temperature and wind speed have been taken less than and greater than 300 W m^{-2} , $28 \text{ }^{\circ}\text{C}$ and 6 m s^{-1} , respectively.

Supplementary table

Table 3.4: The average \pm standard deviation of the mixing ratios of NMHCs (ppbv) measured over open ocean and coastal regions, and for daytime and nighttime over the Arabian Sea.

S.No.	Ocean	Month / Year	Ethene Avg ppb	Ethene std ppb	Propene Avg ppb	Propene std ppb	Refernces
1	Peruvian upwelling zone	Jul-1982	4	-	0.45	-	Greenberg & Zimmerman, 1984
2	Equatorial Pacific	Dec-1982	0.88	-	0.49	-	Greenberg et al. 1984
3	Western Indian Ocean	Apr-1985	21	-	11	-	Bonsang et al. 1988
4	mid-Atlantic	Mar/Apr 1987	0.058	0.026	-	-	Koppman et al. 1992
5	Hao Atoll	May-Jun 1987	2.4	-	1.7	-	Bonsang et al. 1992
6	Mace Head	Apr/May 1997	21	-	25.1	-	Lewis, et al. 2001
7	Northwest Indian Ocean	Apr-2000	0.223	0.123	0.095	0.045	Warneke & De Gouw, 2001
8	Sub-Antarctic	Jan-Feb 2002	0.162	0.06	0.046	0.021	Bonsang, et al. 2008
9	Bay of Bengal	Sept/Oct 2002	0.299	0.166	0.129	0.053	Sahu et al. 2010
10	Bay of Bengal	Feb-2003	0.188	0.039	0.099	0.032	Sahu et al. 2010
11	Bay of Bengal	Mar-Apr 2006	0.196	0.154	0.112	0.092	Srivastava et al. 2012
12	Arabian Sea	Apr-May 2006	0.165	0.106	0.132	0.088	Srivastava et al. 2012
13	Mediterian Sea	July-Aug 2017	0.114	0.043	0.012	0.008	Bourtsoukidis et al., 2019
14	Gulf of Oman	July-Aug 2017	13.33	-	1.684	-	Bourtsoukidis et al. 2019
15	Arabian Gulf	July-Aug 2017	3.58	-	0.556	-	Bourtsoukidis et al. 2019
16	Red Sea South	July-Aug 2017	0.108	0.317	0.022	0.065	Bourtsoukidis et al. 2019
17	North West Arabian Sea	July-Aug 2017	0.09	0.045	0.012	0.008	Bourtsoukidis et al. 2019
18	Arabian Sea	Apr-May 2017	8.9	3.4	3.8	1.3	Present study

Chapter 4

Work3

Chapter 5

Work4

Chapter 6

Summary and Future Directions

6.1 Summary

•

Chapter 7

Appendix

Chiral Magnetic effects

7.1 Title of second appendix

Bibliography

- [1] D. A. Exton, T. J. McGenity, M. Steinke, D. J. Smith, and D. J. Suggett, *Uncovering the volatile nature of tropical coastal marine ecosystems in a changing world*, *Global change biology* **21** no. 4 1383–1394.
- [2] A. Guenther, *Biological and chemical diversity of biogenic volatile organic emissions into the atmosphere*, *ISRN Atmospheric Sciences* **2013**.
- [3] J. Laothawornkitkul, J. E. Taylor, N. D. Paul, and C. N. Hewitt, *Biogenic volatile organic compounds in the earth system*, *New Phytologist* **183** no. 1 27–51.
- [4] J. Peñuelas and M. Staudt, *Bvocs and global change*, *Trends in plant science* **15** no. 3 133–144.
- [5] C. Plass-Dülmer, A. Khedim, R. Koppmann, F. Johnen, J. Rudolph, and H. Kuosa, *Emissions of light nonmethane hydrocarbons from the atlantic into the atmosphere*, *Global biogeochemical cycles* **7** no. 1 211–228.
- [6] M. Ratte, O. Bujok, A. Spitz, and J. Rudolph, *Photochemical alkene formation in seawater from dissolved organic carbon: Results from laboratory experiments*, *Journal of Geophysical Research: Atmospheres* **103** 5707–5717.
- [7] A. Guenther, X. Jiang, C. Heald, T. Sakulyanontvittaya, T. Duhl, L. Emmons, and X. Wang, *The model of emissions of gases and aerosols from nature version 2.1 (MEGAN2. 1): an extended and updated framework for modeling biogenic emissions*, .

- [8] G. Myhre, D. Shindell, F.-M. Bréon, W. Collins, J. Fuglestvedt, J. Huang, D. Koch, J.-F. Lamarque, D. Lee, and B. Mendoza, *Anthropogenic and natural radiative forcing*, *Climate change* **423** 658–740.
- [9] N.-A. Fuchs, *Evaporation and droplet growth in gaseous media*. Elsevier.
- [10] J. D. Fuentes, M. Lerdau, R. Atkinson, D. Baldocchi, J. Bottenheim, P. Ciccioli, B. Lamb, C. Geron, L. Gu, A. Guenther, et al., *Biogenic hydrocarbons in the atmospheric boundary layer: a review*, *Bulletin of the American Meteorological Society* **81** no. 7 1537–1576.
- [11] J. Lelieveld, T. M. Butler, J. N. Crowley, T. J. Dillon, H. Fischer, L. Ganzeveld, H. Harder, M. G. Lawrence, M. Martinez, D. Taraborrelli, and J. Williams, *Atmospheric oxidation capacity sustained by a tropical forest*, *Nature* **452** 737.
- [12] S. L. Shaw, B. Gantt, and N. Meskhidze, *Production and emissions of marine isoprene and monoterpenes: a review*, *Advances in Meteorology* **2010**.
- [13] N. Meskhidze and A. Nenes, *Phytoplankton and cloudiness in the southern ocean*, *Science* **314** no. 5804 1419–1423.
- [14] N. M. Donahue and R. G. Prinn, *Nonmethane hydrocarbon chemistry in the remote marine boundary layer*, *Journal of Geophysical Research: Atmospheres* **95** 18387–18411.
- [15] S. Liu, S. McKeen, and M. Trainer, *Impacts of biogenic non-methane hydrocarbons on the tropospheric chemistry*, vol. 28, p. 419.
- [16] T. Groene, *Biogenic production and consumption of dimethylsulfide (dms) and dimethylsulfoniopropionate (dmsp) in the marine epipelagic zone: a review*, *Journal of Marine Systems* **6** no. 3 191–209.
- [17] J. Lovelock, *Natural halocarbons in the air and in the sea*, *Nature* **256** 193.

- [18] J. J. B. W. A. K. Y. L. J. L. T. M. B. M. G. E. L. Mungall, Jonathan P. D. Abbatt, *Microlayer source of oxygenated volatile organic compounds in the summertime marine arctic boundary layer*, .
- [19] A. Orlikowska and D. E. Schulz-Bull, *Seasonal variations of volatile organic compounds in the coastal baltic sea*, *Environ. Chem.* **6** no. 6 495–507.
- [20] H. Singh, Y. Chen, A. Tabazadeh, Y. Fukui, I. Bey, R. Yantosca, D. Jacob, F. Arnold, K. Wohlfrom, and E. Atlas, *Distribution and fate of selected oxygenated organic species in the troposphere and lower stratosphere over the atlantic*, *Journal of Geophysical Research: Atmospheres* **105** 3795–3805.
- [21] C. Plass-Dülmer, R. Koppmann, M. Ratte, and J. Rudolph, *Light nonmethane hydrocarbons in seawater*, *Global Biogeochemical Cycles* **9** 79–100.
- [22] M. Ratte, C. Plass-Dülmer, R. Koppmann, J. Rudolph, and J. Deng, *Production mechanism of c2-c4 hydrocarbons in seawater: Field measurements and experiments*, *Global Biogeochemical Cycles* **7** no. 2 369–378.
- [23] T. Saito, K. Kawamura, T. Nakatsuka, and B. J. Huebert, *In situ measurements of butane and pentane isomers over the subtropical north pacific*, *Geochemical Journal* **38** no. 5 397–404.
- [24] S. Arnold, D. Spracklen, J. Williams, N. Yassaa, J. Sciare, B. Bonsang, V. Gros, I. Peeken, A. Lewis, and S. Alvain, *Evaluation of the global oceanic isoprene source and its impacts on marine organic carbon aerosol*, *Atmospheric Chemistry and Physics* **9** no. 4 1253–1262.
- [25] A. Baker, S. Turner, W. Broadgate, A. Thompson, G. McFiggans, O. Vesperini, P. Nightingale, P. Liss, and T. Jickells, *Distribution and sea-air fluxes of biogenic trace gases in the eastern atlantic ocean*, *Global Biogeochemical Cycles* **14** no. 3 871–886.

- [26] A. Lewis, J. McQuaid, N. Carslaw, and M. Pilling, *Diurnal cycles of short-lived tropospheric alkenes at a north atlantic coastal site*, *Atmospheric Environment* **33** no. 15 2417–2422.
- [27] E. Liakakou, M. Vrekoussis, B. Bonsang, C. Donousis, M. Kanakidou, and N. Mihalopoulos, *Isoprene above the eastern mediterranean: Seasonal variation and contribution to the oxidation capacity of the atmosphere*, *Atmospheric Environment* **41** no. 5 1002–1010.
- [28] J. Rudolph and F. Johnen, *Measurements of light atmospheric hydrocarbons over the atlantic in regions of low biological activity*, *Journal of Geophysical Research: Atmospheres* **95** 20583–20591.
- [29] T. Saito, Y. Yokouchi, and K. Kawamura, *Distributions of c2–c6 hydrocarbons over the western north pacific and eastern indian ocean*, *Atmospheric environment* **34** no. 25 4373–4381.
- [30] B. Bonsang, M. Kanakidou, and G. Lambert, *NMHC in the marine atmosphere: Preliminary results of monitoring at amsterdam island*, *Journal of Atmospheric Chemistry* **11** no. 1 169–178.
- [31] W. J. Broadgate, P. S. Liss, and S. A. Penkett, *Seasonal emissions of isoprene and other reactive hydrocarbon gases from the ocean*, *Geophysical Research Letters* **24** no. 21 2675–2678.
- [32] N. Gist and A. Lewis, *Seasonal variations of dissolved alkenes in coastal waters*, *Marine chemistry* **100** no. 1 1–10.
- [33] P. Warneck and J. Williams, *The atmospheric Chemist's companion: numerical data for use in the atmospheric sciences*. Springer Science & Business Media.
- [34] M. Madhupratap, S. P. Kumar, P. M. A. Bhattathiri, M. D. Kumar, S. Raghukumar, K. K. C. Nair, and N. Ramaiah, *Mechanism of the biological response to winter cooling in the northeastern arabian sea*, *Nature* **384** 549.

- [35] R. R. Nair, V. Ittekkot, S. J. Manganini, V. Ramaswamy, B. Haake, E. T. Degens, B. N. Desai, and S. Honjo, *Increased particle flux to the deep ocean related to monsoons*, *Nature* **338** 749.
- [36] A. Singh and R. Ramesh, *Environmental controls on new and primary production in the northern indian ocean*, *Progress in Oceanography* **131** 138–145.
- [37] M. G. Sreeush, V. Valsala, S. Pentakota, K. V. S. R. Prasad, and R. Murtugudde, *Biological production in the indian ocean upwelling zones–part 1: refined estimation via the use of a variable compensation depth in ocean carbon models*, *Biogeosciences* **15** no. 7 1895–1918.
- [38] F. Azam, G. F. Steward, D. C. Smith, and H. W. Ducklow, *Significance of bacteria in carbon fluxes in the arabian sea*, *Proceedings of the Indian Academy of Sciences-Earth and Planetary Sciences* **103** no. 2 341–351.
- [39] V. Eyring, H. Köhler, J. Van Aardenne, and A. Lauer, *Emissions from international shipping: 1. the last 50 years*, *Journal of Geophysical Research: Atmospheres* **110**.
- [40] S. B. D. Øyvind Endresen Ivar S. A. Isaksen Gjermund Gravir Eirik Sørgrå d, *Environmental impacts of the expected increase in sea transportation, with a particular focus on oil and gas scenarios for norway and northwest russia*, *Journal of Geophysical Research: Atmospheres* **112**.
- [41] S. Lal and M. G. Lawrence, *Elevated mixing ratios of surface ozone over the arabian sea*, *Geophysical Research Letters* **28** no. 8 1487–1490.
- [42] B. S. Ingole, S. Sautya, S. Sivadas, R. Singh, and M. Nanajkar, *Macrofaunal community structure in the western indian continental margin including the oxygen minimum zone*, *Marine Ecology* **31** no. 1 148–166.
- [43] D. A. Hansell and E. T. Peltzer, *Spatial and temporal variations of total organic carbon in the arabian sea*, *Deep Sea Research Part II: Topical Studies in Oceanography* **45** no. 10 2171–2193.

- [44] R. R. Draxler and G. Hess, *An overview of the hysplit 4 modelling system for trajectories*, *Australian meteorological magazine* **47** no. 4 295–308.
- [45] L. Cheng and J. Zhu, *2017 was the warmest year on record for the global ocean*, *Advances in Atmospheric Sciences* **35** no. 3 261–263.
- [46] D. Capone, J. P. Zehr, H. Paerl, B. Bergman, and E. Carpenter, *Trichodesmium, a globally significant marine cyanobacterium*, *Science* **276** 1221–1229.
- [47] A. J. Poulton, M. C. Stinchcombe, and G. D. Quartly, *High numbers of trichodesmium and diazotrophic diatoms in the southwest indian ocean*, *Geophysical Research Letters* **36** no. 15.
- [48] N. Gandhi, A. Singh, S. Prakash, R. Ramesh, M. Raman, M. Sheshshayee, and S. Shetye, *First direct measurements of n₂ fixation during a trichodesmium bloom in the eastern arabian sea*, *Global Biogeochemical Cycles* **25** no. 4.
- [49] T. Jabir, V. Dhanya, Y. Jesmi, M. Prabhakaran, N. Saravanane, G. Gupta, and A. Hatha, *Occurrence and distribution of a diatom-diazotrophic cyanobacteria association during a trichodesmium bloom in the southeastern arabian sea*, *International Journal of Oceanography* **2013**.
- [50] L. M. Momper, B. K. Reese, G. Carvalho, P. Lee, and E. A. Webb, *A novel cohabitation between two diazotrophic cyanobacteria in the oligotrophic ocean*, *The Isme Journal* **9** 882.
- [51] P. S. Liss, C. A. Marandino, E. E. Dahl, D. Helmg, E. J. Hintsa, C. Hughes, M. T. Johnson, R. M. Moore, J. M. Plane, and B. Quack, *Short-lived trace gases in the surface ocean and the atmosphere*, in *Ocean-Atmosphere Interactions of Gases and Particles*, pp. 1–54. Springer, Berlin, Heidelberg.

- [52] L. Sahu, S. Lal, and S. Venkataramani, *Impact of monsoon circulations on oceanic emissions of light alkenes over bay of bengal*, *Global Biogeochemical Cycles* **24** no. 4.

List of Publications

1.

